

1 Determination of respiration and photosynthesis fractionation
2 factorsefficients for atmospheric dioxygen inferred from a
3 vegetation-soil-atmosphere analog of the terrestrial biosphere in
4 closed chambers

5
6 Clémence Paul¹, Clément Piel², Joana Sauze², Nicolas Pasquier¹, Frédéric Prié¹, Sébastien Devidal²,
7 Roxanne Jacob¹, Arnaud Dapoigny¹, Olivier Jossoud¹, Alexandru Milcu^{2,3}, Amaëlle Landais¹

8
9 ¹Laboratoire des Sciences du Climat et de l'Environnement, LSCE/IPSL, CEA-CNRS-UVSQ, Université Paris-
10 Saclay, 91191 Gif-sur-Yvette, France

11 ²Ecotron Européen de Montpellier (UAR 3248), Univ Montpellier, Centre National de la Recherche Scientifique
12 (CNRS), Campus Baillarguet, Montferrier-sur-Lez, France

13 ³Centre d'Ecologie Fonctionnelle et Evolutive, Univ Montpellier, CNRS, Univ Paul Valéry, EPHE, IRD, Montpellier,
14 France

15
16 Correspondence: Clémence Paul (clemence.paul@lsce.ipsl.fr)

17

18 Abstract

19 The isotopic composition of dioxygen in the atmosphere is a global tracer which depends on the
20 biosphere flux of dioxygen toward and from the atmosphere (photosynthesis and respiration) as well
21 as exchanges with the stratosphere. When measured in fossil air trapped in ice cores, the relative
22 concentration of ¹⁶O, ¹⁷O and ¹⁸O of O₂ can be used for several applications such as ice core dating and
23 past global productivity reconstruction. However, there are still uncertainties about the accuracy of
24 these tracers as they depend on the integrated isotopic fractionation–discrimination of different
25 biological processes of dioxygen production and uptake, for which we currently have very few
26 independent estimates. –Here we determined the respiration and photosynthesis fractionation
27 factorsefficients for atmospheric dioxygen from experiments carried out in a replicated vegetation-
28 soil-atmosphere analog of the terrestrial biosphere in closed chambers with growing *Festuca*
29 *arundinacea*. The values for ¹⁸O discrimination during soil respiration and dark respiration in
30 leavesleave are equal to -12.3 ± 1.7 ‰ and -19.1 ± 2.4 ‰, respectively. We also found a value for
31 terrestrial photosynthetic fractionation–isotopic discrimination equal to $+3.7 \pm 1.3$ ‰. This last

32 estimate suggests that the contribution of terrestrial productivity in the Dole effect may have been
33 underestimated in previous studies.

34

35 1. Introduction

36 The oxygen cycle represents one of the most important biogeochemical ~~cycle~~ on Earth as: oxygen
37 is the second most important gaseous component in the atmosphere. Oxygen is an essential
38 component for life on Earth as it is consumed by all aerobic organisms through respiration and
39 produced by autotrophic organisms through photosynthesis.

40 The analysis of the oxygen isotopic composition classically expressed as $\delta^{18}\text{O}$ and $\delta^{17}\text{O}$ of O_2 in air
41 bubbles trapped in ice cores is currently used to provide information on the variations of the low
42 latitude water cycle and the productivity of the biosphere during the Quaternary (Bender et al., 1994;
43 Luz et al., 1999; Malaizé et al., 1999; Severinghaus et al., 2009; Blunier et al., 2002; Landais et al., 2010).
44 $\delta^{18}\text{O}$ of O_2 is also a very useful proxy for ice core dating through the resemblance of its variations with
45 the variations of precession or summer insolation in the northern hemisphere (Shackleton, 2000;
46 Dreyfus et al., 2007). These tracers are however complex and their interpretation relies on the precise
47 knowledge of the various fractionation factors in the oxygen cycle.

48 First, interpreting the relationship between~~interpretation of variations of~~ $\delta^{18}\text{O}$ of O_2 (or $\delta^{18}\text{O}_{\text{atm}}$)
49 variations in the old air trapped in ice core air and their term of low latitude water cycle (e.g.
50 Severinghaus et al., 2009; Landais et al., 2010; Seltzer et al., 2017) is still debated because of the
51 multiple~~multiplicity of the~~ processes involved. Dole et al. (1954) showed~~has shown~~ that the $\delta^{18}\text{O}_{\text{atm}}$ is
52 enriched compared to the $\delta^{18}\text{O}$ of water of the global ocean (taken here as the Vienna Standard Mean
53 Ocean Water, VSMOW) with a value of 23.88 ‰ (Barkan and Luz, 2005). This Dole effect is the result
54 of several isotopic discriminations~~fractionations caused by~~in the biosphere-biotic processes that enrich
55 the $\delta^{18}\text{O}_{\text{atm}}$ relative to the oceanic values of water $\delta^{18}\text{O}$. First measurements~~one. Measurements~~ have
56 shown that the photosynthesis itself is not associated with a strong isotopic
57 discrimination~~fractionation~~ and produces oxygen with an isotopic composition which is close to the
58 isotopic composition of the consumed water (Vinogradov et al., 1959; Stevens et al., 1975; Guy et al.,
59 1993; Helman et al., 2005; Luz & Barkan, 2005). This is in contrast to the early results of Dole and Jenks
60 (1959) who proposed a photosynthetic isotopic discrimination for plants and algae of 5%. Vinogradov
61 et al. (1959) challenged the results of Dole and Jenks (1944) by explaining that the ^{18}O enrichment of
62 O_2 during their photosynthesis experiments is the result of contamination by atmospheric O_2 and
63 respiration. Guy et al. (1993) studied the photosynthetic isotopic discrimination on spinach thylakoids,

64 cyanobacteria (*Anacystis nidulans*) and diatoms (*Phaeodactylum tricorutum*) and found only a slight
65 isotopic discrimination of 0.3‰ which they considered negligible. Luz and Barkan (2005) also
66 corroborates this idea by studying photosynthetic isotopic discrimination on *Philodendron* and did not
67 obtain a ^{18}O enrichment of the O_2 produced. This absence of isotopic discrimination can be
68 theoretically explained by the process of O_2 generation within photosynthesis (photosystem II)
69 involving water oxidation by the oxygen evolving complex (Tcherkez and Farquhar, 2007). For the
70 oceanic biosphere, the isotopic composition of O_2 produced by photosynthesis (Guy et al., 1993). For
71 the oceanic biosphere, the isotopic composition of O_2 is very close to the isotopic composition of the
72 ocean. However, in terrestrial biosphere the $\delta^{18}\text{O}$ of water split during consumed by photosynthesis
73 (leaf water) is highly variable both spatially and temporally because of the decrease of $\delta^{18}\text{O}$ of meteoric
74 water toward higher latitudes (Dansgaard, 1974) and the enrichment in heavy isotopes in leaf water
75 during evaporation (Dongmann et al., 1974). The mean $\delta^{18}\text{O}$ enrichment of leaf water isotopic
76 composition has been estimated between within + 4.5 and + 6 ‰ with respect to the isotopic
77 composition of ~~the~~ mean global ocean water (Bender et al., 1994; Hoffmann et al., 2004). On top of
78 this enrichment, the terrestrial and oceanic Dole effects are mostly explained by the respiratory
79 isotopic discrimination of the order of magnitude of + 18 ‰ (Bender et al., 1994).

80 Because of the isotopic enrichment in leaf water, the terrestrial Dole effect has been initially estimated
81 to be 5 ‰ higher than the oceanic Dole effect and $\delta^{18}\text{O}_{\text{atm}}$ used to estimate changes in the balance
82 between land and marine productivity (Wang et al., 2008; Bender et al., 1994; Hoffmann et al., 2004).
83 However, the evidence by Eisenstadt et al. (2010) of isotopic discrimination up to + 6 ‰ for marine
84 phytoplankton photosynthesis rather suggests that the marine and terrestrial Dole effects are of the
85 same order of magnitude. More specifically, Eisenstadt et al. (2010) determined several
86 photosynthetic isotopic discrimination values depending on the phytoplankton studied
87 (*Phaeodactylum tricorutum* = 4.5 ‰, *Nannocloropsis sp.* = 3 ‰, *Emiliania huxleyi* = 5.5 ‰ and
88 *Chlamydomonas reinhardtii* = 7‰). If marine and terrestrial Dole effects are similar, then in this case,
89 the past variations of $\delta^{18}\text{O}_{\text{atm}}$ cannot be attributed to different proportions of terrestrial or marine Dole
90 effects. They would better ~~would~~ be related to low latitude water cycle influencing the leaf water $\delta^{18}\text{O}$
91 consumed by photosynthesis and then the $\delta^{18}\text{O}$ of O_2 produced by this process (with a larger flux (most
92 important in the low latitude vegetated regions). This is supported by orbital and millennial variations
93 of $\delta^{18}\text{O}_{\text{atm}}$ in phase with calcite $\delta^{18}\text{O}$ in Chinese speleothem, a proxy strongly related to the intensity of
94 hydrological cycle in the South-East Asia (Severinghaus et al., 2009; Landais et al., 2010; Extier et al.,
95 2018). The aforementioned studies show that qualitative and quantitative interpretation of $\delta^{18}\text{O}_{\text{atm}}$
96 relies strongly on the estimate of O_2 fractionation factors in the biological cycle but data to constrain

97 the fractionation factors associated with respiration and photosynthesis for the different ecosystems
98 are sparse.

99 In addition to the use of $\delta^{18}\text{O}_{\text{atm}}$, the combination of $\delta^{17}\text{O}$ and $\delta^{18}\text{O}$ of O_2 provides a way to quantify
100 variations in past global productivity (Luz et al., 1999). This method relies on the fact that O_2 -
101 fractionating processes in the stratosphere and within the biosphere lead to different relationships
102 between $\delta^{17}\text{O}$ and $\delta^{18}\text{O}$ of O_2 . ~~Oxygen~~The biosphere fractionating processes are mass-dependent such
103 ~~that the ^{17}O enrichment is about half the ^{18}O enrichment relative to ^{16}O .~~ On the contrary, oxygen is
104 fractionated in a mass-independent manner in the stratosphere producing approximately equal ^{17}O
105 and ^{18}O enrichments (Luz et al., 1999). On the contrary, the biosphere fractionating processes are
106 mass-dependent such that the ^{17}O enrichment is about half the ^{18}O enrichment relative to ^{16}O . We
107 thus define a $\Delta^{17}\text{O}$ anomaly as:

108

$$109 \quad \Delta^{17}\text{O} = \ln(1 + \delta^{17}\text{O}) - 0.516 \times \ln(1 + \delta^{18}\text{O}) \quad (1)$$

110

111 $\Delta^{17}\text{O}$ of O_2 is equal to 0 by definition in the present-day troposphere (the standard for isotopic
112 composition of atmospheric oxygen is the present-day atmospheric value). $\Delta^{17}\text{O}$ of O_2 is negative in
113 the stratosphere and ~~increases~~increase in biosphere productivity leads to an increase of $\Delta^{17}\text{O}$ of O_2 . As
114 for the interpretation of $\delta^{18}\text{O}_{\text{atm}}$, the quantitative link between $\Delta^{17}\text{O}$ of O_2 and biosphere productivity
115 depends on the exact fractionation factors associated with biosphere processes (Brandon et al., 2020).

116 Several studies have been conducted to estimate the fractionation factors during biosphere processes
117 of O_2 production and consumption. These fractionation factors are then implemented in global
118 modeling approaches involving the use of models of global vegetation and oceanic biosphere for
119 interpretation of $\Delta^{17}\text{O}$ of O_2 and $\delta^{18}\text{O}_{\text{atm}}$ in term of environmental parameters (Landais et al., 2007;
120 Blunier et al., 2012; Reutenauer et al., 2015; Brandon et al., 2020). Most of the fractionation factors
121 used in these modeling approaches were obtained from studies conducted at the cell level:
122 cyanobacterium (Helman et al., 2005), *E. coli* (Stolper et al., 2018), microalgae (Eisenstadt et al., 2010).
123 In these studies, the underlying assumption is that the fractionation factor associated with O_2
124 measured at the cell level can be applied at the ecosystem scale. Yet, results from studies conducted
125 at a larger scale, e.g. at the soil scale by Angert et al. (2001) found a global terrestrial respiratory
126 $^{18}\text{O}/^{16}\text{O}$ of O_2 discrimination for soil microorganisms varying between - 12 ‰ and - 15 ‰. This is lower
127 than the - 18 ‰ discrimination classically used for respiration, with diffusion in soil playing a role in
128 addition to the biological respiration isotopic discrimination. Angert and Luz (2001) also showed using

129 experiments on roots of Philodendron plants and wheat seedlings that the respiratory discrimination
130 of a soil with roots is lower (about - 12‰) than the - 18‰ discrimination associated with the dark
131 respiration. This is due to the low O₂ concentration in roots whose presence favors a slower
132 diffusion.~~biological respiration fractionation.~~ Later, Angert et al. (2003) found an even larger spread of
133 O₂ isotopic discrimination in soil and showed that temperate and boreal soils have higher
134 ~~fractionation~~isotopic discrimination, respectively - 17.8 ‰ and - ~~22.5 ‰.~~22.5 ‰, ~~because they engage~~
135 ~~the AOX (alternative oxidase) pathway which strongly discriminates ¹⁸O, unlike tropical soils (- 10.8 ‰).~~
136 ~~These contrasting results show the interest of making measurements at a larger scale than at the cell~~
137 ~~level to correctly interpret global variations of the isotopic composition of oxygen.~~

138 It has been suggested that the strong discrimination observed for boreal and temperate soils is due to
139 the involvement of the alternative oxidase pathway (AOX, Bendall and Bonner, 1971) in addition to
140 the usual COX respiratory pathway. In the COX respiration pathway, present in the majority in plants,
141 the cytochrome oxidase enzyme catalyzes the oxygen reduction reaction. In the AOX pathway, the
142 oxidation of ubiquinol molecules is directly coupled to the reduction of oxygen. Guy et al. (2005)
143 showed that, for green tissues, the respiratory discrimination of the AOX pathway is much higher (- 31
144 ‰) than the one of the COX pathway (- 21 ‰). Similarly, Ribas-Carbo et al. (1995) found a higher
145 respiratory discrimination in phytoplankton that engage the AOX pathway (- 31 ‰) relative to bacteria
146 that engage the COX pathway (- 24 ‰).

147 Other studies had attempted to investigate the different respiratory discriminations in the light (dark
148 respiration, Mehler reaction and photorespiration). As during the light period, dark respiration can be
149 inhibited (70 % inhibition found by Tcherkez et al. (2017) and Keenan et al. (2019)), so that the other
150 O₂ consuming processes are important to consider. The Mehler reaction reduces oxygen to form a
151 superoxide ion which is converted to hydrogen peroxide (H₂O₂) in photosystem I and then further
152 converted to water (Mehler, 1951). Photorespiration is the result of the oxygenase activity of Rubisco
153 (Sharkey, 1998). This enzyme can oxidize ribulose-1,5-bisphosphate with an oxygen molecule O₂. This
154 reaction causes a loss of CO₂ incorporation, thus decreasing the photosynthetic yield (Bauwe et al.,
155 2010). Guy et al. (1993) first found a photorespiratory discrimination of - 21.7 ‰ and a ¹⁸O/¹⁶O
156 discrimination of - 15.3 ‰ for the Mehler reaction. Later, on a study performed on pea, Helman et al.
157 (2005) found ¹⁸O/¹⁶O discriminations of - 21.3 ‰ and - 10.8 ‰ respectively for photorespiration and
158 Mehler reaction.

159 The above presented state of the art shows contrasting results for the determination of fractionation
160 factors for the different photosynthesis and O₂ uptake processes, thus underlining the importance of
161 performing new measurements to correctly interpret global variations of the isotopic composition of

oxygen. Moreover, because there may be a difference between the fractionation factors at the cell level and at a broader level as shown for dark respiration in soil, we will favor here an approach at the scale of a terrarium including plant and soil.

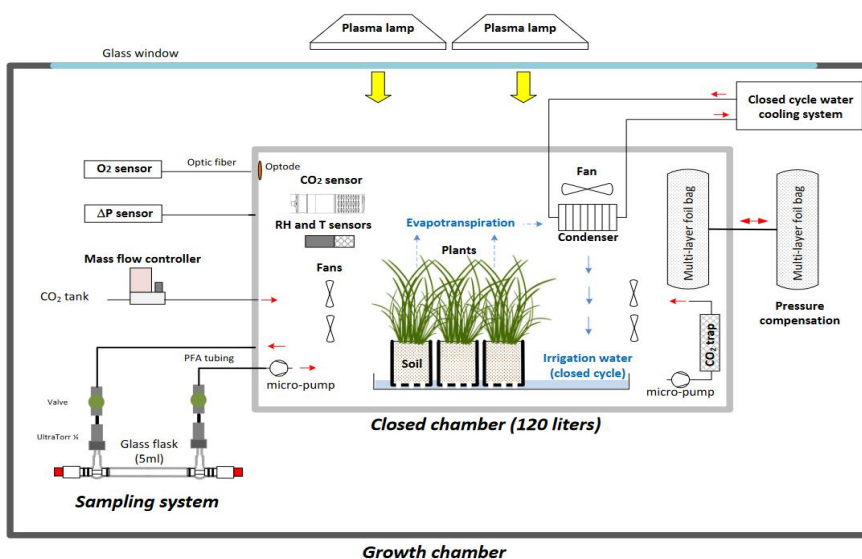
In this study we developed a simplified vegetation-soil-atmosphere ~~simplified~~ analog of the terrestrial biosphere in closed chamber of 120 dm^3 liters with the aim of estimating the fractionation ~~factors~~ coefficients of atmospheric dioxygen due to soil respiration, plant respiration and photosynthesis. With this setup we carried out several experimental runs with soil only and soil with plants in order to estimate the ~~fractionation~~ isotopic discrimination of the different compartments and check values obtained at the cell level. The implications for our interpretation of the Dole effect are also discussed.

2. Material and Methods

2.1. Growth chamber and closed system

2.1.1. Plant growth and experimental setup

a)



b)



178

179 **Fig.1. A vegetation-soil-atmosphere analog of the terrestrial biosphere in a closed chamber. (a)**
 180 **Schematic of the closed chamber setup used for the terrestrial biosphere model.** The 120 ~~dm³liters~~
 181 gas tight closed chamber containing a terrestrial biosphere analogue is enclosed in a larger growth
 182 chamber from the Ecotron ~~MicrocosmsMicrocosms~~ platform. Main environmental parameters inside
 183 the closed chamber are actively controlled and monitored: temperature (T), light intensity, CO₂,
 184 relative humidity (RH), pressure differential (ΔP). The water cycle in the closed chamber is shown in
 185 blue. **(b) Photograph of the closed chamber used in the experiment with *Festuca arundinacea*.**

186

187 Seeds of *Festuca arundinacea* (Schreb.), also commonly called tall fescue, were first sown in a
 188 commercial potting soil (Terreau universel, Botanic, France. Composition: black and blond peat, wood
 189 fibre, green compost and vermicompost manure, organic and organo-mineral fertilizers and
 190 micronutrient fertilizers). During 15 to 20 days, they were then placed in a growth chamber of the
 191 Microcosms experimental platform of the European Ecotron of Montpellier
 192 (<https://www.ecotron.cnrs.fr>) under diurnal light-dark cycles ([Table S1](#)),
 193 air temperature set at 20 °C (T_{air}), air relative humidity (RH) at 80 % and CO₂ atmospheric concentration close to ambient air
 194 (concentration of CO₂ = 400 ppm).

195 Twelve pots (8 cm × 8 cm × 12 cm with 180 to 200 g of dry soil) containing
 196 ~~approximately~~ 25 to 30 ~~fescue~~-mature fescue plants were used for each experimental
 197 run. All plants were placed in a plastic tray filled with tap water, inside an airtight transparent chamber
 198 manufactured from welded polycarbonate (10 mm wall thickness and 120 liters volume) similar to the
 199 chambers used by Milcu et al. (2013) (Fig. 1). The sealing of the closed chamber was checked before
 200 each experiment using helium.

201 To control temperature and light intensity inside the closed chamber, this ~~smaller chamber~~ was
202 placed in a larger controlled environment growth chamber. Light was provided by two plasma lamps
203 (GAVITA Pro 300 LEPO2; GAVITA) with PAR = 200 $\mu\text{mol}\cdot\text{m}^{-2}\cdot\text{s}^{-1}$ and air temperature inside the closed
204 chamber was regulated at 19 ± 1 °C by adjusting the growth chamber temperature.

205 The closed chamber (Fig. 1) was used as a closed gas exchange system with controlled, and
206 continuously monitored, environmental parameters. Air and soil temperature (CTN 35, Carel), air
207 relative humidity (PFmini72, Michell instrument, USA) and CO₂ atmospheric concentration (GMP343,
208 Vaisala, Finland) were measured and recorded using the growth chamber datalogger (sampling rate =
209 1 min). O₂ concentration was continuously monitored using an optical sensor (Oxy1-SMA, Presens,
210 Germany). Because precise O₂ concentration are determined in our samples by mass spectrometry
211 (see next section), the measurements of the Oxy1-SMA were only used as a control during the
212 experiment. The measured O₂ value for atmospheric air was adjusted to 20.9% before each sequence
213 of experiments and the same adjustment (offset) was then applied to the O₂ record during the
214 following sequence.

215 Air relative humidity was regulated between 80 % and 90 % using a heat exchanger (acting as a
216 condenser) connected to a closed cycle water cooling system. The condenser was positioned in a way
217 to create a ~~water-closed~~ water cycle in the biological chamber (water vapor from evapotranspiration
218 ~~was condensed~~condense back into irrigation water). In order to keep the CO₂ mixing ratio close to 400
219 ~~ppm~~400ppm during the light periods, photosynthetic CO₂ uptake was compensated with injections of
220 pure CO₂ using a mass flow controller (F200CV, Bronkhorst, The Netherlands). During the dark periods,
221 a soda lime trap connected to a micro-pump (NMS 020B, KNF, Germany) was used to remove the
222 excess CO₂ coming from respiration. CO₂ atmospheric concentration during the night was kept below
223 200 ppm.

224 To ensure atmospheric pressure stability in the closed chamber, a pressure compensation system,
225 made of two connected 10 liters gas tight bags (~~Restek multi-layer~~polyvinyl fluoride foil gas
226 sampling bag~~bags~~, Restek, USA), was installed. Each bag was half full of atmospheric air, the first one
227 was installed in the closed chamber while the second one was outside this chamber. This way, each
228 bag ~~inflated~~inflates or ~~deflated~~deflates in response to pressure ~~variations caused~~variation either
229 ~~by~~due to O₂ or CO₂, uptake or release. The pressure difference between the closed chamber and the
230 atmosphere was regularly measured using a differential sensor (FD A602-~~S1K~~Almemo~~S1K~~Almemo,
231 Ahlborn, Germany).

232 Finally, the enclosed air was mixed and considered homogeneous using seven brushless fans.

233

234 2.1.2. Gas sampling

235

236 To measure the isotopic composition along the experiment, small samples of gas were collected in 5
237 mL glass flasks, made of two Louwers H.V. glass valves (1-way bore 9mm Ref. LH10402008, Louwers
238 Hanique, The Netherlands) welded together. Those flasks, previously evacuated, were mounted on
239 PFA tubing (1/4th) using two 1/4th UltraTorr fitting (SS-4-UT-9, Swagelok, USA). Two manual valves (SS-
240 4H, Swagelok, USA) were also installed on the PFA tubes to open or close the circuit. A micro-pump
241 (NMS 20B, KNF, Germany) was finally turned on during air sampling to ensure closed chamber
242 atmosphere circulation through the flask. The flow rate was equal to 1.6 L/min.

243

244 2.2. Isotopic measurements

245 2.2.1. Water extraction from leaf and isotopic analysis

246 After each experiment, the plant leaves were collected, placed in airtight flasks and immediately frozen
247 at - 20°C for at least 24 hours to make sure there was minimal loss of water through vaporization when
248 the vial was opened later. The extraction of water from leaves was done according to the procedure
249 detailed in Alexandre et al. (2018). The vial was fixed onto a cryogenic extraction line and was first
250 ~~immersed~~immersed in a liquid nitrogen Dewar to prevent any sublimation of the water. The water
251 extraction line was emptied of most of its air (< 10⁻⁵ Pa). Once this pressure ~~was has been~~
252 pump was turned off and a valve was closed in order to keep a constant static void within the system.
253 The “reception” vial was then immersed in a liquid nitrogen Dewar ~~{~~which will act as a water trap
254 ~~whilst}~~and the sample vial ~~for the was immersed in~~ water was then transferred to a water bath
255 maintained at 75°C. The system was kept in these conditions for no less than six hours, so that all the
256 water present in the leaf and stems was extracted. Afterwards, in order to remove all of the organic
257 compounds of the extracted water, an active charcoal was placed in the extracted water and left under
258 agitation for the night.

259 For analysis of $\delta^{17}\text{O}$ and $\delta^{18}\text{O}$ of water, leaf water was converted to O_2 using a fluorination line for
260 reaction of H_2O with CoF_3 heated to 370°C at LSCE. The isotopic composition of the dioxygen was
261 measured ~~an by~~ IRMS equipped with dual inlet (Thermo Scientific MAT253 mass spectrometer). The
262 standard that was chosen was an O_2 standard calibrated against VSMOW. The precision was 0.015 ‰
263 for $\delta^{17}\text{O}$, 0.010 ‰ for $\delta^{18}\text{O}$ and 6 ppm for $\Delta^{17}\text{O}$ (Eq. (1)), for more details, refer to Landais et al. (2006).

264 The values of $\delta^{18}\text{O}$ and $\delta^{17}\text{O}$ of leaf water measured with respect to VSMOW are then expressed with
265 respect to the isotopic composition of dioxygen in atmospheric air (classical standard for $\delta^{18}\text{O}$ and $\delta^{17}\text{O}$
266 of O_2 measurements). No consensus has been reached for the values of $\delta^{18}\text{O}$ and $\delta^{17}\text{O}$ of O_2 in
267 atmospheric air with respect to $\delta^{17}\text{O}$ and $\delta^{18}\text{O}$ of H_2O of VSMOW. These differences are most probably
268 to be attributed to the different analytical techniques used for preparing and measuring the samples

(Yeung et al., 2018; Wostbrock et al., 2021). In our case, because we use a similar set-up with the one developed by Barkan and Luz (2003) for the analyses of the triple isotopic composition of O₂ in air (cf next section), we have chosen to base our calculation on their estimates. In this study, we have thus chosen the value of 23.88 ‰ for δ¹⁸O of O₂ values with respect to VSMOW following (Barkan and Luz, 2005). As for the δ¹⁷O of O₂ value with respect to VSMOW value, we use two different possible estimates from these authors, either 12.03 ‰ (Luz and Barkan, 2011) or 12.08 ‰ (Barkan and Luz, 2005). We acknowledge that because of the absence of consensus, slightly different values could be obtained for the fractionation factors determined in this study if a different choice is made for the reference values of δ¹⁸O and δ¹⁷O of O₂ in atmospheric air with respect to δ¹⁷O and δ¹⁸O of H₂O of VSMOW.

2.2.2. O₂ purification and isotopic analysis

The air samples collected in the closed chambers were transported to LSCE for analyses of the isotopic composition of O₂. The flasks were connected on a semi-automatic separation line inspired from Barkan and Luz (2003) which was made up of 8 ports in which 2 standards (outside air) and 6 samples were analyzed daily (Brandon et al., 2020). After pumping the whole line, the air was circulated through a water trap (ethanol at -100°C) and then through a carbon dioxide trap immersed in liquid nitrogen at -196°C. After collection of the gas samples on a molecular sieve trap cooled at -196°C, a helium flow carried it through a chromatographic column which was immersed in a water reservoir at 0°C to separate the dioxygen and the argon from the dinitrogen. After separation of the dioxygen and argon from helium, the gas was collected in a stainless-steel manifold immersed in liquid helium at -269°C.

After collection, the samples were analyzed by the IRMS previously mentioned for leaf water analyses. The following ratios were measured: ¹⁸O/¹⁶O, ¹⁷O/¹⁶O and O₂/Ar (as an indicator of the O₂ concentration because Ar is an inert gas). δ¹⁷O and δ¹⁸O of O₂ each sample were obtained through 3 series of 24 dual inlet measurements against a standard made of O₂ and Ar. This sequence was followed by 2 peak jumping analyses of the O₂/Ar ratio including separate measurements of the O₂ and Ar signals for both the standard and the sample. The uncertainty associated with each measurement was obtained from the standard deviation of the three runs and from the repeated peak jumping

measurement for δO₂/Ar which was defined by
$$\left[\frac{\left(\frac{n(O_2)}{n(Ar)} \right)_{sample}}{\left(\frac{n(O_2)}{n(Ar)} \right)_{standard}} - 1 \right] * 1000$$
, and $n(O_2)$ is the number of moles of O₂ and $n(Ar)$ the number of moles of Ar. The uncertainty values for Δ¹⁷O, δ¹⁸O and δO₂/Ar were respectively 10 ppm, 0.05 ‰ and 0.5 ‰.

299 Each day, we performed measurements of the ~~dioxygenoxygen~~ isotopic composition and O₂/Ar ratio
300 on two samples of outside air which is the standard for the isotopic composition of O₂ (Hillaire-Marcel
301 et al., 2021). So that the calibrated δ¹⁸O value for our sample was calculated as in equation 2:

$$\delta^{18}O_{calibrated} = \left[\frac{(\delta^{18}O_{measured}/1000)+1}{(\delta^{18}O_{outsideair}/1000)+1} - 1 \right] \times 1000 \quad (2)$$

305 2.3. Experimental runs

306 2.3.1. General strategy

307 Our goal was to calculate the fractionation factor associated with δ¹⁷O and δ¹⁸O for soil respiration,
308 dark leaf respiration and photosynthesis using the microcosm described above. In order to quantify
309 the fractionation factors, we needed to work in closed and controlled conditions. Given the volume of
310 the closed chamber (120 dm³L, hence about 1.12 moles of O₂) and the order of magnitude of dark
311 respiration (order of magnitude of 0.08 μmol O₂ s⁻¹ for soil respiration) and net photosynthetic fluxes
312 (order of magnitude of 0.45 μmol O₂ s⁻¹) inside the chamber, we calculated that experiments should
313 last from ~~323~~ days to more than 2 weeks so that more than one tenth of the O₂ in the chamber can be
314 recycled by the plant and soil. This recycling ~~allows~~allowed the creation of sufficiently large isotopic
315 signals (especially Δ¹⁷O of O₂) to be detected and measured. We ~~had~~ set up two different experiments
316 in the closed chamber, each experiment being repeated 3 or 4 times to characterize the~~address~~
317 experimental repeatability of the system.

318 The first experiment (repeated 4 times, i.e. in 4 sequences) aimed at studying the fractionation
319 ~~factorsefficients~~ during soil respiration. The second experiment (repeated 3 times, i.e. in 3
320 sequences, each sequence being divided into several periods with or without light) aimed at studying
321 the fractionation ~~factorsefficients~~ during dark respiration and photosynthesis of plants.

322 Prior to the aforementioned experiments, measurements were carried out on a closed empty chamber
323 to check the absence of leaks as well as the absence of isotopic fractionation (Table ~~S2S4~~).

325 2.3.2. Soil respiration experiment

326 To conduct the soil respiration experiment, 2.6 kg of soil (*Terreau universel, Botanic*) were placed in 12
327 different pots. The light was turned off during this experimental run (Table S1). We decided not to
328 apply any diurnal cycles during dark respiration experimentations for two reasons. First, we wanted to

329 prevent the development of algae, mosses or any photosynthetic organisms in the chamber. Secondly,
330 it was easier to optimize temperature control as the light radiation could increase the temperature
331 inside the closed chamber. During this dark period, CO₂ from soil respiration accumulates in the
332 biological closed chamber. To have a stable concentration of CO₂ during the whole dark period, the
333 CO₂ was trapped using soda lime. Four sequences were performed with respective durations of 53, 51,
334 43 and 36 days.

335

336 2.3.3. Photosynthesis and dark respiration experiment

337 We used the same soil with plants (*Festuca arundinacea*) grown before the start of the three
338 sequences of the photosynthesis and dark respiration experiment. In order to obtain a significant
339 change of the Δ¹⁷O of O₂ signal in our ~~closed~~ 120 dm³ chambers, the 3 experiments were run
340 ~~for~~ during 1 to 2 months. CO₂ level was controlled ~~to 400 ppm~~ by a CO₂ trap and CO₂ injections. This
341 was done to ensure that the CO₂ in the chamber did not reach levels too far from the atmospheric
342 composition as this could have affected the physiology of the plant. This could have affected the
343 physiology of the plant. The ~~light cycle~~ ~~enlightenment~~ was controlled to alternate between day
344 (photosynthesis and respiration) and night conditions (respiration) (Table S1).

345 The values of the leaf water measurements are presented in supplementary Table S3. Because the
346 experiments had to be carried in a closed chamber, we could not sample leaves during the experiment
347 and only got a value at the end of each sequence. Nevertheless, we could compare the isotopic
348 composition of the irrigation and soil water at the start and at the end of the experiment.

349

350 2.4. Quantification of fractionation ~~factor~~ ~~se~~ ~~efficient~~s

351 We detail below how we used the results from our experiments to quantify the associated
352 fractionation ~~factor~~ ~~se~~ ~~efficient~~s. Notations used below are gathered in Table 1.

353 The isotopic fractionation ~~factor~~ ~~se~~ ~~efficient~~ of oxygen is expressed through the fractionation
354 ~~factor~~ ~~se~~ ~~efficient~~ α.

355

$$356 \quad {}^{18}\alpha = \frac{{}^{18}R_{product}}{{}^{18}R_{substrat}} \quad {}^{18}\alpha = \frac{R^{18}O_{product}}{R^{18}O_{substrat}}$$

357 (3)

358

359 ~~where~~Where α is the fractionation ~~factor~~coefficient and $^{18}R_{R^{18}O}$ is the ratio of the concentration

360 $^{18}R = \frac{n(^{18}O)}{n(^{16}O)}$ ~~$R^{18}O = \frac{n(^{18}O)}{n(^{16}O)}$~~ with n the number of moles of O_2 containing ^{18}O or ^{16}O . $^{18}R_{R^{18}O}$ is

361 linked to the $\delta^{18}O$ value through:

362

363
$$\delta^{18}O = \left(\frac{^{18}R_{sample}}{^{18}R_{standard}} - 1 \right) \left(\frac{R^{18}O_{sample}}{R^{18}O_{standard}} - 1 \right) \times 1000$$

364 (4)

365

366 The isotopic discrimination is related to the isotopic fractionation ~~factor~~coefficient through:

367
$$^{18}\epsilon = ^{18}\alpha - 1$$
 (5)

368 The same equations (3), (4) and (5) can be proposed for $\delta^{17}O$ and the relationship between the
 369 fractionation ~~factor~~coefficients $^{17}\alpha$ and $^{18}\alpha$ is written as:

370
$$\theta = \frac{\ln ^{17}\alpha}{\ln ^{18}\alpha}$$
 (6)

371

372 2.4.1. Soil respiration

373 Respiration is associated with isotopic fractionation. The light isotopes, ^{16}O , are more easily integrated
 374 by microorganisms than the heavy isotopes, ^{18}O , which hence remain in the atmosphere. We express
 375 the fractionation ~~factor~~coefficient for soil respiration as:

376

377
$$^{18}\alpha_{soil_respi} = \frac{^{18}R_{respired} \cdot R^{18}O_{breathed}}{^{18}R_{air} \cdot R^{18}O_{air}}$$
 (7)

378

379 In our experiment, the respiratory process took place in a closed reservoir so that we could calculate
 380 the fractionation ~~factor~~coefficients from the evolution of the concentration and isotopic composition
 381 of dioxygen in the chamber. The ~~evolution of the~~ number of molecules of dioxygen in the air of the
 382 closed chamber, $n(O_2)$, between time t and time $t+dt$ can be written as:

383

384
$$n(O_2)_t - n(O_2)_{t+dt} = n(O_2)_t + dn(O_2)$$
 (8)

385

386

387 with $dn(O_2)$ the number of dioxygen molecules respired during the time period dt . A similar equation
 388 can be written for the number of dioxygen molecules containing ^{18}O remaining in the air of the
 389 chamber:

390

$$391 \quad {}^{18}R_{t+dt} \times n(O_2)_{t+dt} = {}^{18}R_t \times n(O_2)_t + {}^{18}R_t \times \alpha_{soil_respi} \times dn(O_2) \quad (9)$$

393

394 The evolution of the isotopic ratio of oxygen, ^{18}R , between time t and time $t+dt$ can be written as:

395

$$396 \quad {}^{18}R_{t+dt} = {}^{18}R_t + d^{18}R \quad (10)$$

397

398 Combining equations Eq. (8), and Eq. (9) and (10), neglecting the second order term $d^{18}R_t \times$
 399 $dn(O_2)_t$ and integrating from t_0 (starting time of the experiment when the chamber is closed) to t
 400 leads to:

401

$$402 \quad {}^{18}\epsilon_{soil_respi} = {}^{18}\alpha_{soil_respi} - 1 = \frac{\ln\left(\frac{\frac{\delta^{18}O_{t+1}}{1000}}{\frac{\delta^{18}O_{t0}}{1000}}\right)}{\ln\left(\frac{n(O_2)_t}{n(O_2)_{t0}}\right)}$$

$$403 \quad (11) \quad \frac{\ln\left(\frac{\frac{R^{18}O_{t+1}}{1000}}{\frac{R^{18}O_{t0}}{1000}}\right)}{\ln\left(\frac{n(O_2)_t}{n(O_2)_{t0}}\right)} \quad (10)$$

404

405 Because Since argon is an inert gas, we can link $\frac{n(O_2)_t}{n(O_2)_{t0}}$ to $\delta\left(\frac{O_2}{Ar}\right)$, so that:

406

$$407 \quad \frac{n(O_2)_t}{n(O_2)_{t0}} = \frac{\frac{\delta\left(\frac{O_2}{Ar}\right)_{t+1}}{1000}}{\frac{\delta\left(\frac{O_2}{Ar}\right)_{t0}}{1000}} \quad (12)$$

408

409

410 2.4.2. Dark respiration

411 In order to calculate the isotopic fractionation associated with soil and plant respiration during dark
 412 period, we followed the same calculation as for the soil respiration (section 2.4.1). In this case, we
 413 selected only night periods from each sequence of the photosynthesis and dark respiration
 414 experiment.

415

416 **2.4.3. Photosynthesis**

417 During photosynthesis, the oxygen atoms in the dioxygen produced by the plant comes from the
418 oxygen atom of water consumed by photosynthesis in the leaves so that the fractionation
419 factor~~coefficient~~ during photosynthesis can be expressed as:

420

$$^{18}\alpha_{\text{photosynthesis}} = \frac{^{18}R_{\text{produced } O_2}}{^{18}R_{lw}}$$

421

$$(13) \frac{R^{18}O_{\text{produced } O_2}}{R^{18}O_{lw}} \quad (12)$$

422

423

424 where~~Where~~ *lw* stands for leaf water.

425 For our study of *Festuca arundinacea* we consider that the water in the mesophyll layer can be
426 represented by bulk leaf water.

427

428 Photosynthesis occurs during the light periods. However, it should be noted that dark respiration,
429 photorespiration and Mehler reaction occur at the same time. In a first approach, we did the
430 assumption that respiration rates remain the same during the light and dark periods. This
431 assumption is probably true for soil respiration since flux of heterotrophic dark respiration is not
432 expected to change for different light conditions if the other environmental drivers (e.g. humidity,
433 temperature, soil organic matter) are constant. However, autotrophic dark respiration is expected to
434 decrease during light periods compared to dark periods. As a consequence, we present sensitivity
435 tests to the dependence of a vanishing dark respiration of leaves during the dark period in Table S4.

436

437 Thus, at each stage, dioxygen~~Mehler's reaction (Mehler, 1951) occur at the same time. Thus, at each~~
438 stage, oxygen is both produced by photosynthesis and consumed by the aforementioned O₂ uptake
439 processes (hereafter *total_respi*) by the plant according to the mass conservation equation:

440

$$n(O_2)_{t+dt} = n(O_2)_{t+dt} + dn_{\text{total_respi}} + dn_{\text{photosynthesis}}$$

441

442 (14)~~13~~

443

444 where dn_{total_respi} is the number of molecules of O_2 consumed by dark respiration, photorespiration
 445 and MehlerMehler's reaction between time t and $t+dt$, and $dn_{photosynthesis}$ is the number of
 446 molecules of O_2 produced by photosynthesis between t and $t+dt$.

447
 448 The budget for ^{18}O of O_2 can be written as:

$$\begin{aligned}
 &^{18}R_{t+dt} \times R^{18}O_t \times \frac{n(O_2)_t}{n(O_2)_{t0}} = R^{18}O_{t+dt} \times \frac{n(O_2)_{t+dt}}{n(O_2)_{t0}} = ^{18}R_t \times \frac{n(O_2)_t}{n(O_2)_{t0}} + ^{18}R_t R^{18}O_{t+dt} \times \\
 &^{18}\alpha_{total_respi} \times \frac{dn_{total_respi}}{n(O_2)_{t0}} + ^{18}R_{lw} \times R^{18}O_{lw} \times ^{18}\alpha_{photosynthesis} \times \frac{dn_{photosynthesis}}{n(O_2)_{t0}} \\
 &\hspace{15em} \underline{\hspace{15em}} \hspace{15em} (15)-(14)
 \end{aligned}$$

449
 450
 451 where $^{18}\alpha_{total_respi}$ is the fractionation factorscoefficients associated with each O_2 consuming
 452 process periods throughout the whole experiment.

453
 454 We introduced the normalized fluxes of photosynthesis and total respiration as:

$$F_{photosynthesis} = \frac{dn_{photosynthesis}}{n(O_2)_{t0} \times dt} \hspace{15em} \underline{\hspace{15em}}$$

$$(16) \left| \frac{dn_{photosynthesis}}{n(O_2)_{t0} \times dt} \right| \hspace{15em} (15)$$

457
 458 And,

$$F_{total_respi} = \frac{dn_{total_respi}}{n(O_2)_{t0} \times dt} \hspace{15em} = \left| \frac{dn_{total_respi}}{n(O_2)_{t0} \times dt} \right|$$

$$\hspace{15em} \underline{\hspace{15em}} (16)$$

459
 460 as well as,

$$aR^{18} = \left| \frac{R^{18}O_t}{dt} \right| \hspace{15em} (17)$$

$$a^{18}R = \frac{d^{18}R}{dt} \hspace{15em} (18)$$

461
 462 This led to the following expression of $^{18}\alpha_{photosynthesis}$:-

$$\begin{aligned}
 &^{18}\alpha_{photosynthesis} = \\
 &\frac{n(O_2)_t / n(O_2)_{t0} \times a^{18}R + ^{18}R_t \times (F_{photosynthesis} + F_{total_respi} - ^{18}\alpha_{total_respi} \times F_{total_respi})}{^{18}R_{lw} \times F_{photosynthesis}} = \\
 &\frac{-aR^{18} + F_{photosynthesis} - F_{total_respi} + ^{18}\alpha_{total_respi} \times F_{total_respi}}{R^{18}O_{lw} \times F_{photosynthesis}} \hspace{15em} (18)
 \end{aligned}$$

(19)

This equation can be simplified at t=0 for $^{18}R_t = ^{18}R_{t0} = 1$ and $n(O_2)_t = n(O_2)_{t0}$:

$^{18}\alpha_{photosynthesis}$ depends on the values of $^{18}\alpha_{total_respi}$ and of F_{total_respi} , themselves dependent on the values of $^{18}\alpha_{Mehler}$, $^{18}\alpha_{dark_respi}$ and F_{dark_respi} (fractionation factor associated with Mehler reaction), F_{Mehler} (flux of oxygen related to Mehler reaction), $^{18}\alpha_{photorespi}$ (fractionation factor associated with photorespiration) and $F_{photorespi}$ (photorespiration flux of oxygen). These last 4 parameters could not be determined in our global experiment. Our determination of $^{18}\alpha_{photosynthesis}$ will thus rely on assumptions for the estimations of $^{18}\alpha_{Mehler}$, F_{Mehler} , $^{18}\alpha_{photorespi}$ and $F_{photorespi}$.

To separate the $^{18}\alpha_{dark_respi}$ from the other fractionation factors, we defined:

$$^{18}\alpha_{total_respi} = ^{18}\alpha_{photorespi} \times f_{photorespi} + ^{18}\alpha_{Mehler} \times f_{Mehler} + ^{18}\alpha_{dark_respi} \times f_{dark_respi}$$

(2019)

with

$$F_{total_respi} = F_{dark_respi} + F_{photorespi} + F_{Mehler}$$

(2120)

f indicates the fraction of the total oxygen uptake flux corresponding to each process (dark respiration, photorespiration and Mehler's reaction) so that:

$$f_{dark_respi} + f_{photorespi} + f_{Mehler} = 1$$

(2221)

$$F_{dark_respi} = f_{dark_respi} \times F_{total_respi} \tag{22}$$

$$F_{photorespi} = f_{photorespi} \times F_{total_respi} \tag{23}$$

508

509 $F_{Mehler} = f_{Mehler} \times F_{total_respi}$ _____

510 ~~(25).~~ _____ ~~(24)~~

511

512 In the absence of further constraints, we used here as first approximation the global values from
 513 Landais et al. (2007) for f_{dark_respi} (0.6), $f_{photorespi}$ (0.3) and f_{Mehler} (0.1). Values for $\alpha_{photorespi}$ and
 514 α_{Mehler} were ~~also taken from Landais et al. (2007)~~ based on the most recent estimates of Helman et
 515 al. (2005).

516

517 **Table 1. List of variables used to quantify fractionations and their definitions.** * means either oxygen
 518 17 or oxygen 18.

Symbol	DefinitionDescription	Origin of the value
* α	Fractionation factor <u>coefficient</u>	
* α_{dark_respi}	Fractionation factor <u>coefficient</u> of soil and plant respiration during night period <u>period</u> during photosynthesis and respiration experiment	<u>Determined by our study</u>
* $\alpha_{dark_leaf_respi}$ *α_{dark}	Fractionation factor <u>coefficient</u> of leaf respiration of leaf <u>during night period</u> during photosynthesis and respiration experiment	<u>Determined by our study</u>
* α_{Mehler}	Fractionation factor <u>coefficient</u> associated with Mehler respiration	<u>Value from Helman et al. (2005)</u>
* $\alpha_{photorespi}$	Fractionation factor <u>coefficient</u> associated with photorespiration	<u>Value from Helman et al. (2005)</u>
* $\alpha_{photosynthesis}$	Fractionation factor <u>coefficient</u> associated with photosynthesis	<u>Determined by our study</u>
* α_{soil_respi}	Fractionation factor <u>coefficient of soil respiration</u> associated with soil respiration experiment	<u>Determined by our study</u>
* α_{total_respi}	Fractionation factor <u>coefficient</u> associated with total respiration during light period	<u>Determined by our study</u>
* ϵ	Isotopic discrimination	
* ϵ_{dark_respi}	Isotopic discrimination of soil and plant respiration during night period <u>period during photosynthesis and respiration experiment</u>	<u>Determined by our study</u>

$\epsilon_{dark_leaf_respi}$	Isotopic discrimination of leaf respiration during night periods	Determined by our study
$\epsilon_{photosynthesis}$	Isotopic discrimination associated with photosynthesis	Determined by our study
ϵ_{soil_respi}	Isotopic discrimination of soil respiration associated with soil respiration experiment	Determined by our study
θ	Ratio of $\ln(^{17}\alpha)$ to $\ln(^{18}\alpha)$	
θ_{dark_respi}	Ratio of $\ln(^{17}\alpha_{dark_respi})$ to $\ln(^{18}\alpha_{dark_respi})$	Determined by our study
$\theta_{dark_leaf_respi}$	Ratio of $\ln(^{17}\alpha_{dark_leaf_respi})$ to $\ln(^{18}\alpha_{dark_leaf_respi})$	Determined by our study
$\theta_{photosynthesis}$	Ratio of $\ln(^{17}\alpha_{photosynthesis})$ to $\ln(^{18}\alpha_{photosynthesis})$	Determined by our study
θ_{soil_respi}	Ratio of $\ln(^{17}\alpha_{soil_respi})$ to $\ln(^{18}\alpha_{soil_respi})$	Determined by our study
a_N	Linear regression coefficient of the evolution of $n(O_2)$ as a function of time	Determined by our study
a_{R^*O}	Linear regression coefficient of the evolution of R^*O as a function of time	Determined by our study
$dn_{photosynthesis}$	Number of moles of O_2 produced by photosynthesis between t and t+dt	Determined by our study
dn_{total_respi}	Number of moles of O_2 consumed by total respiration during light periods between time t and t+dt	Determined by our study
F_{dark_respi}	Dark respiration flux (normalized vs number of moles of O_2 at the start of the experiment)	Determined by our study
F_{Mehler}	Mehler flux (normalized vs number of moles of O_2 at the start of the experiment)	Determined by our study and Landais et al. (2007)
$F_{photorespi}$	Photorespiration O_2 flux (normalized vs number of moles of O_2 at the start of the experiment)	Determined by our study and Landais et al. (2007)
$F_{photosynthesis}$	Photosynthesis O_2 flux (normalized vs number of moles of O_2 at the start of the experiment)	Determined by our study
F_{total_respi}	Total respiration O_2 flux during light period (normalized vs number of moles of O_2 at the start of the experiment)	Determined by our study
f_{dark_respi}	Fraction of the dioxygen flux corresponding to dark respiration process	Value from Landais et al. (2007)
f_{Mehler}	Fraction of the dioxygen flux corresponding to Mehler process	Value from Landais et al. (2007)

$f_{photorespi}$	Fraction of the dioxygen ^{oxygen} flux corresponding to photorespiration process	<u>Value from Landais et al. (2007)</u>
$n(O_2)$	Number of moles ^{Moles} of O_2	<u>Determined by our study</u>
$*RR^*O$	Ratio of heavy (^{18}O or ^{17}O) isotope to light isotope (^{16}O) <u>of O_2 in air</u>	<u>Determined by our study</u>
$*R_{lw}R^*O_{lw}$	$*RR^*O$ of leaf water	<u>Determined by our study</u>

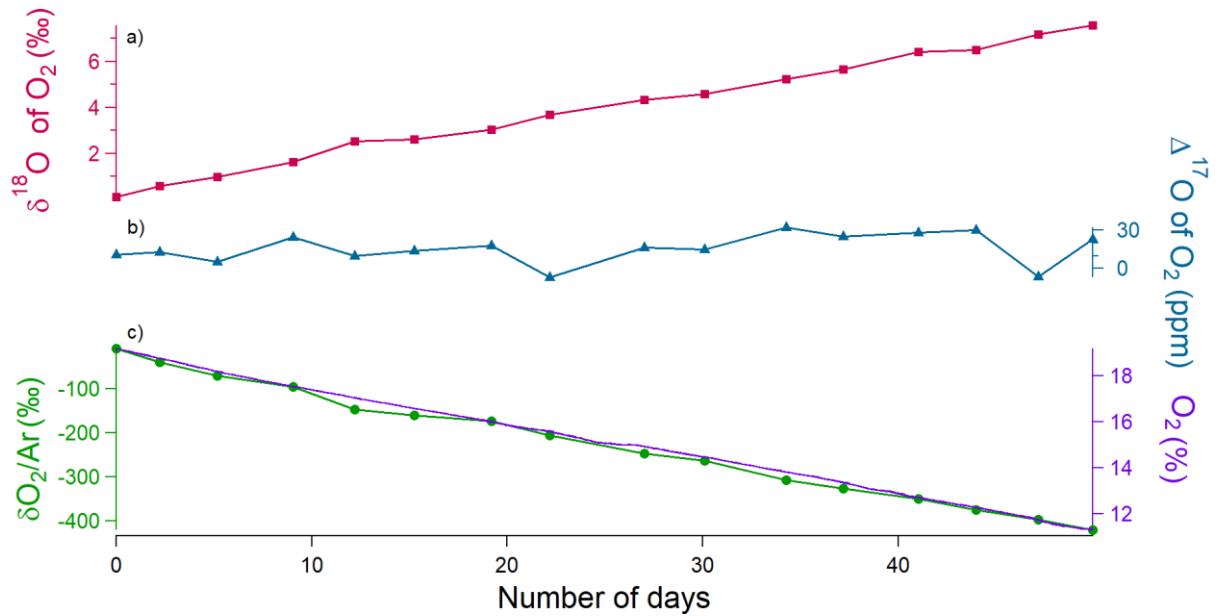
519

520 3.Results

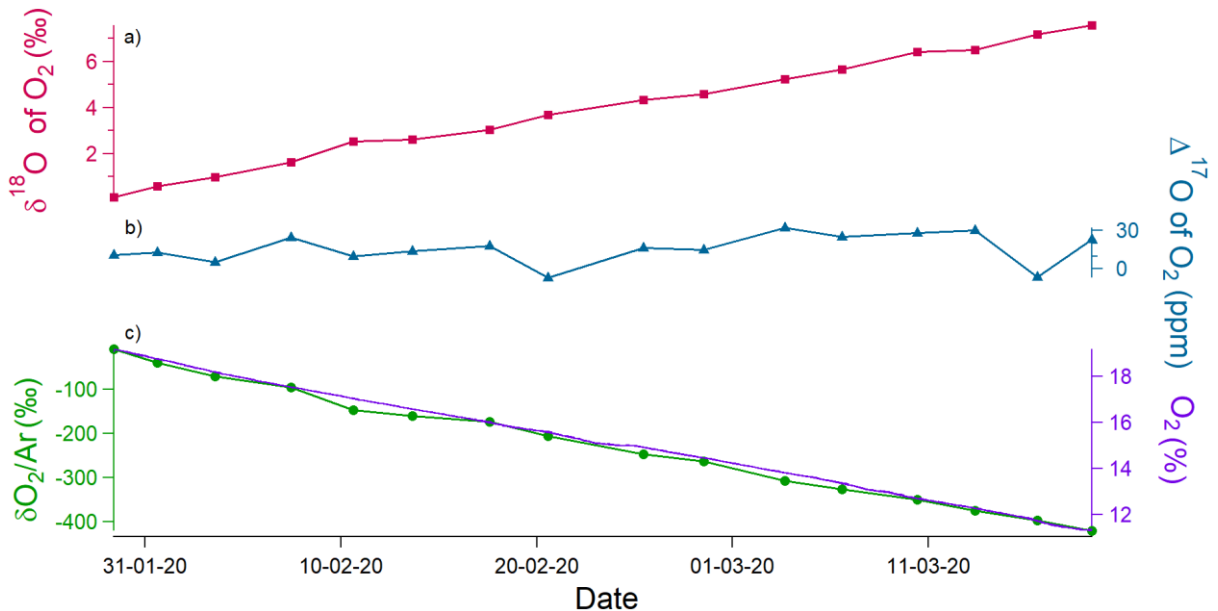
521 3.1. Soil Respiration

522 3.1.1. Experimental data

523



524



525

526

527 **Fig.2. Evolution of the different concentrations and isotopic ratios in the sequence 2 of the soil**
 528 **respiration experiment (day 0 is the beginning of the sequence) in the closed chamber over 51 days.**
 529 **(a) $\delta^{18}\text{O}$ of O₂ (red) variations. (b) $\Delta^{17}\text{O}$ of O₂ (blue) variations. (c) Dioxygen concentration (purple)**
 530 **from the optical sensor and $\delta\text{O}_2/\text{Ar}$ variations (green) measured by IRMS.-**

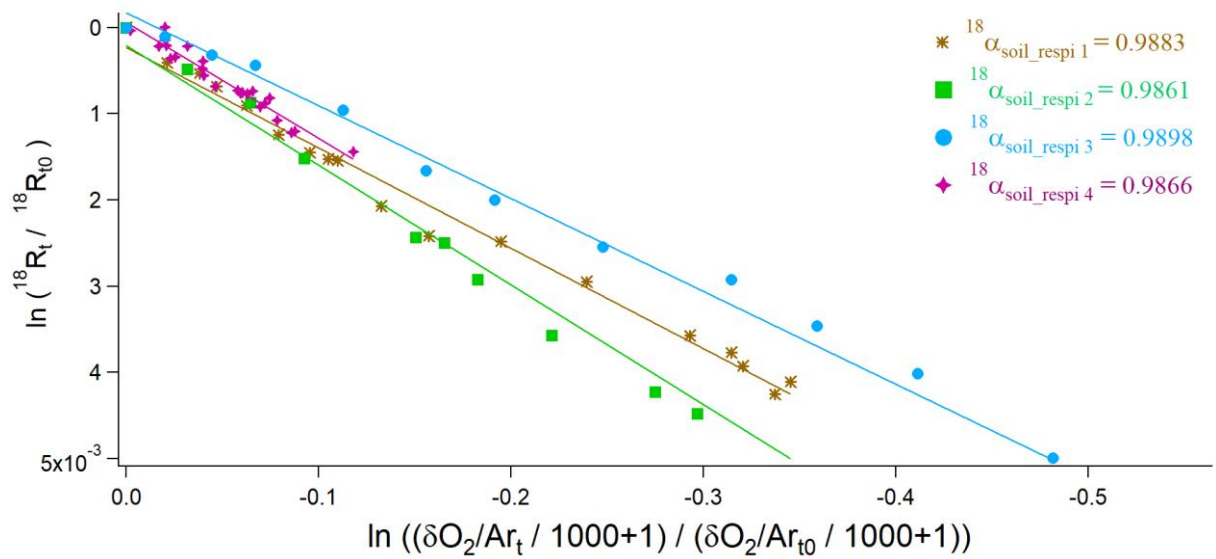
531 During the 4 sequences, the respiration activity led to a decreasing level of the O₂ concentration
 532 measured by the optical sensor or through the $\delta\text{O}_2/\text{Ar}$ evolution from IRMS measurements (Fig. S1).
 533 The comparison of the evolution of the O₂ concentration during the different sequences showed that
 534 respiratory fluxes were different with a maximum factor of 4 between the different sequences (Fig.

535 S1). In parallel to the decrease in O₂ concentration, the δ¹⁸O increased as expected ~~because since~~
536 respiration preferentially consumes the lightest isotopes: over the 51 days of the 2nd soil respiration
537 sequence, we observed a linear decrease of oxygen concentration by more than 5% while δ¹⁸O
538 increased by 8‰ (Fig. 2). A Mann-Kendall ~~test (95%)~~ trend test showed that the Δ¹⁷O of O₂ does not show
539 any statistically significant trend ~~within 95%~~ over the 4 sequences (Fig. S2) (p-values were equal to
540 0.40, 0.08, 0.58, 0.47, respectively).~~S2).~~

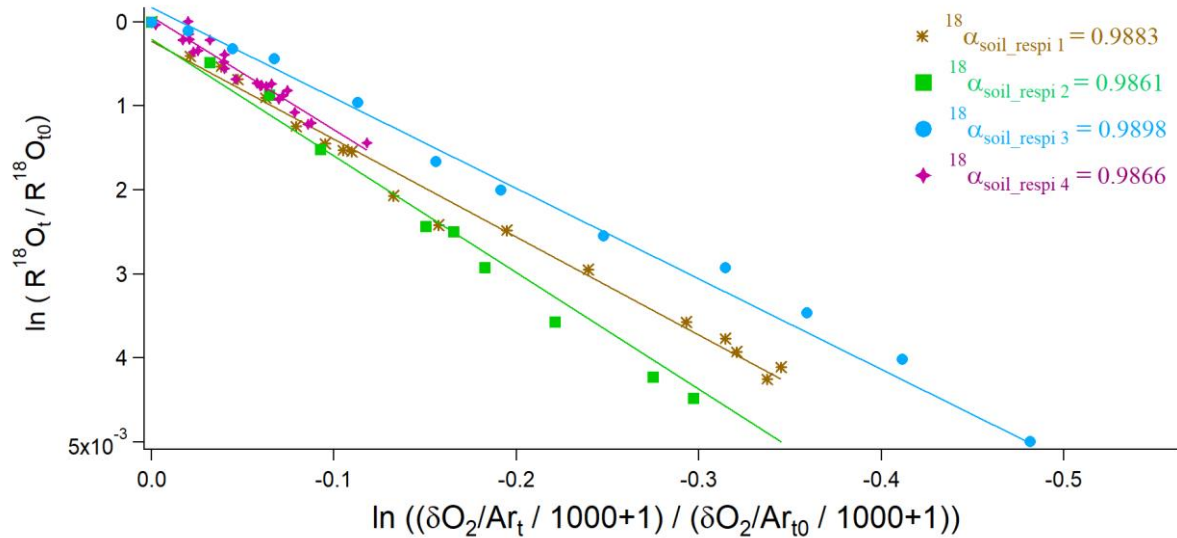
541 3.1.2. Fractionation ~~factors~~ coefficients

542 We used the 15 to 20 samples obtained during each sequence of soil respiration experiment to draw
543 the relative evolution of ~~$\ln(^{18}R_t/^{18}R_{t_0})$~~ ~~$\ln(R^{18}O_t/R^{18}O_{t_0})$~~ vs
544 ~~$\ln((\delta(\frac{O_2}{Ar})_t/1000 + 1)/(\delta(\frac{O_2}{Ar})_{t_0}/1000 + 1))$~~ following Eq. ~~(1140)~~ (Fig. 3). The slope of the
545 corresponding regression line ~~drawn~~ provided the isotopic discrimination $^{18}\epsilon_{soil_respi}$ and hence the
546 fractionation ~~factor~~ efficient $^{18}\alpha_{soil_respi}$ for each sequence. (Table S5S2). It could be observed that
547 despite differences in respiratory fluxes for the different sequences (the standard deviation is equal to
548 50 % of the average flux across sequences; see Table S5), the relationship between δ¹⁸O of O₂ and O₂
549 concentration (or ~~δO_2~~ ~~$\delta O_2/Ar$~~) and hence the calculated fractionation factor associated with
550 respiration, is not much affected. ~~The observed differences between respiratory fluxes could be~~
551 ~~explained by the small variations in organic carbon and by a different development of microbial~~
552 ~~populations during the different experiments.~~

553



554



555

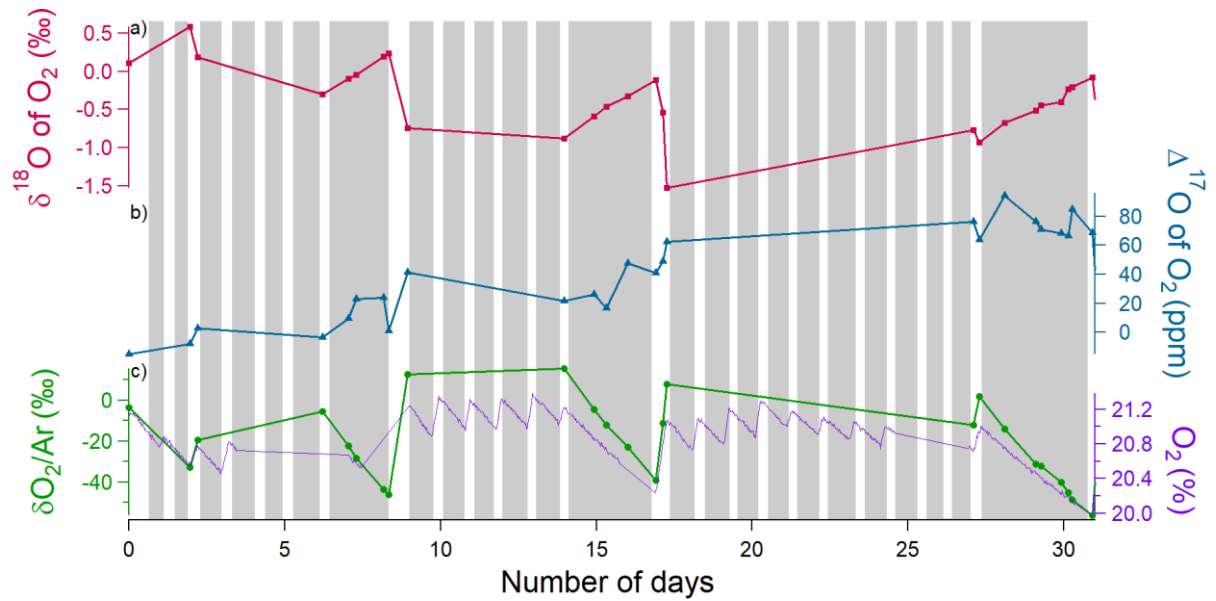
556 **Fig.3 Determination of $^{18}\text{O}/^{16}\text{O}$ fractionation factorsefficients in the 4 respiration sequences.**557 $^{18}\alpha_{soil_respi\ 1}$ (brown), $^{18}\alpha_{soil_respi\ 2}$ (green), $^{18}\alpha_{soil_respi\ 3}$ (blue), $^{18}\alpha_{soil_respi\ 4}$ (purple) are558 **respectively respiratory factorsefficients associated with sequences 1 to 4.**

559 Using the results of the 4 sequences, we determined the values for the mean isotopic discrimination

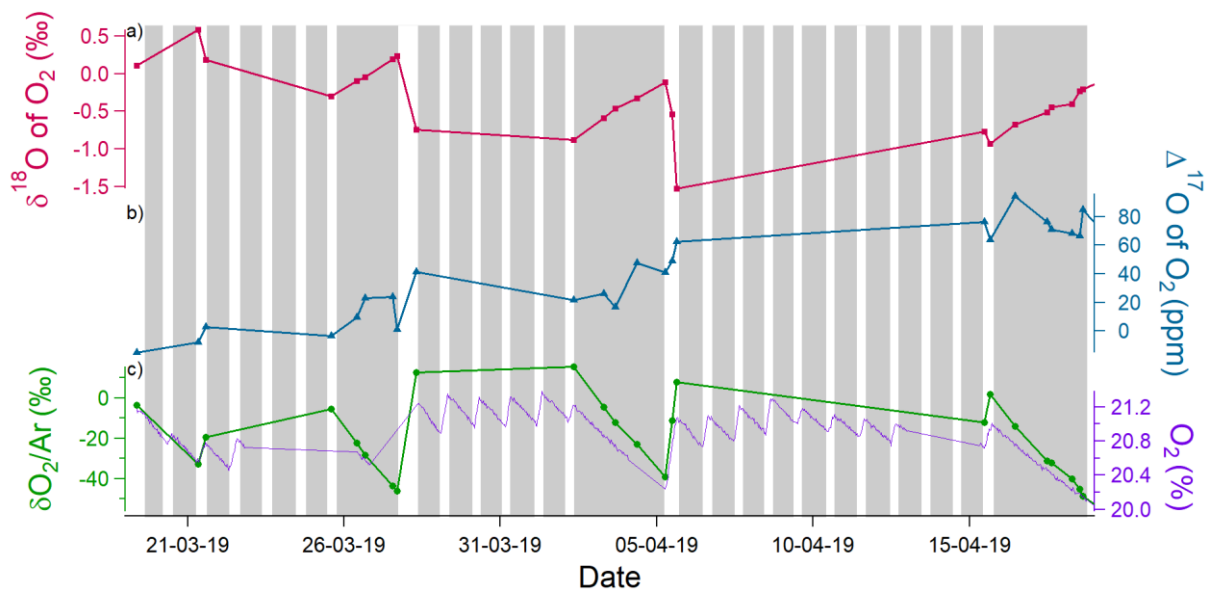
560 $^{18}\epsilon_{soil_respi}$ (-12.3 ± 1.7 ‰), the mean isotopic discrimination $^{17}\epsilon_{soil_respi}$ (-6.4 ± 0.9 ‰) and the561 average $\theta_{soil_respi} \overline{\gamma_{soil_respt}}$ (0.5164 ± 0.0005).

562

563 **3.2. Photosynthesis and dark respiration**564 **3.2.1. Experimental data**



565



566

567

Fig.4. Example of the evolution of the different concentrations and isotopic ratios in the sequence 1 of photosynthesis and dark respiration experiment in the closed chamber over 3130 days (day 0 is the beginning of the sequence). Grey rectangles correspond to night periods and white rectangles to light periods. (a) $\delta^{18}\text{O}$ of O_2 (red) variations. (b) $\Delta^{17}\text{O}$ of O_2 (blue) variations (blue) and regulation of carbon dioxide flux (purple). (c) Dioxygen concentration (purple) from the optical sensor and $\delta\text{O}_2/\text{Ar}$ variations (green) measured by IRMS.

573

574

During the night period~~period without light~~, when only respiration occurred, we observed a decrease in O_2 concentration by 1% within 3 days and a $\delta^{18}\text{O}$ increase by 1-‰ during the same period (Fig. 4). The evolution was qualitatively similar with that of soil respiration experiments with higher fluxes. We observed the same trends for the evolution of $\delta\text{O}_2/\text{Ar}$ during the night ~~During~~ periods as for the respiration experiment. During ~~with~~ light periods, there was a marked decrease in $\delta^{18}\text{O}$ (2 ‰) and a

578

579 marked increase in the fluxflow of oxygen released (1%) during 1 day. ~~This result was consistent with~~
 580 ~~the study of Guy et al. (1993) showing that photosynthesis produces oxygen with the $\delta^{18}\text{O}$ value equal~~
 581 ~~to the $\delta^{18}\text{O}$ of the leaf water, leaf water $\delta^{18}\text{O}$ being lower than atmospheric $\delta^{18}\text{O}$ of O_2 .~~ We observed
 582 the same trends for the evolution of $\delta\text{O}_2/\text{Ar}$ during the night periods as for the respiration experiment.

583

584 The Mann-Kendall test (95%) showed a significative increasing trend of the $\Delta^{17}\text{O}$ of O_2 over sequences
 585 1 and 2 (Fig. S3) (≈ 100 ppm in ~~3130~~ days for sequence 1, ≈ 100 ppm in 40 days for sequence 2) while
 586 ~~there~~ no significant increase of $\Delta^{17}\text{O}$ of O_2 is observed over sequence 3 (Fig. S3).

587

588 3.2.2. Fractionation ~~factors~~coefficients

589 Dark respiration

590 The average of the isotopic discrimination for dark respiration $^{18}\epsilon_{\text{dark_respi}}$ and $^{17}\epsilon_{\text{dark_respi}}$ were
 591 calculated over the 9 night periods and we obtained values of respectively $-17.0 \pm 2.0 \%$ and $-8.5 \pm$
 592 0.8% . The average of $\theta_{\text{dark_respi}}$ ~~$\gamma_{\text{dark_respi}}$~~ during the experiment was equal to 0.5124 ± 0.0084
 593 (details in Table S6S3).

594 The dark respiration of this experiment includes respiration of both soil and leavesleave. Because soil
 595 respiration fractionation ~~factore~~efficient has been determined above, it is possible to estimate here
 596 ~~an estimate of~~ the fractionation ~~factore~~efficient for the dark leafleave respiration and we consider
 597 that respiration rate during dark and light periods do not vary:-

598

$$599 F_{\text{dark_respi}} = F_{\text{soil_respi}} + F_{\text{dark_leaf_respi}} + \cancel{F_{\text{dark_leave_respi}}}$$

600 (2625)

601 ~~And,~~

$$602 ^{18}\alpha_{\text{dark_respi}} = f_{\text{soil_respi}} \times ^{18}\alpha_{\text{soil_respi}} + f_{\text{dark_leaf_respi}} \times ^{18}\alpha_{\text{dark_leaf_respi}} + \cancel{f_{\text{dark_leave_respi}} \times ^{18}\alpha_{\text{dark_leave_respi}}}$$

603 (27) ~~(26)~~

604

605 with $F_{\text{dark_leaf_respi}} / F_{\text{dark_respi}}$ the flux of leafleave respiration during the night, $f_{\text{soil_respi}}$ the
 606 fraction of soil respiration during night periodsperiod ($F_{\text{soil_respi}} / F_{\text{dark_respi}}$) and
 607 $f_{\text{dark_leaf_respi}} / \cancel{f_{\text{dark_leave_respi}}}$ the fraction of dark leafleave respiration during night periodsperiod
 608 ($F_{\text{dark_leaf_leave_respi}} / F_{\text{dark_respi}}$).

609

$$^{18}\alpha_{\text{dark_leaf_respi}} = \frac{^{18}\alpha_{\text{dark_respi}} - f_{\text{soil_respi}} \times ^{18}\alpha_{\text{soil_respi}}}{f_{\text{dark_leaf_respi}}} \quad (28)$$

Thus,

$$\frac{^{18}\alpha_{\text{dark_leaf_respi}}}{^{18}\alpha_{\text{dark_leave_respi}}} = \frac{^{18}\alpha_{\text{dark_respi}} - f_{\text{soil_respi}} \times ^{18}\alpha_{\text{soil_respi}}}{f_{\text{dark_leave_respi}}} \quad (27)$$

613

614 The isotopic discriminations $^{18}\epsilon_{\text{dark_leaf_respi}}$ and $^{18}\epsilon_{\text{dark_leave_respi}}$ and
 615 $^{17}\epsilon_{\text{dark_leaf_respi}}$ and $^{17}\epsilon_{\text{dark_leave_respi}}$ were respectively equals to $-19.1 \pm 2.4 \text{ ‰}$ and $-9.7 \pm 0.9 \text{ ‰}$. The
 616 average of $\theta_{\text{dark_leaf_respi}}$ the gamma value was equal to 0.5089 ± 0.0777 .

617 The standard deviations (1 deviation (σ)) was calculated by a Monte Carlo method from the individual
 618 uncertainties of the $^{18}\alpha_{\text{dark_respi}}$, $^{18}\alpha_{\text{soil_respi}}$, $F_{\text{soil_respi}}$ and $F_{\text{dark_respi}}$.

619

620 Photosynthesis

621 In order to calculate an average value for the fractionation factor/efficient associated with
 622 photosynthesis from Eq. (1918), we first calculated the averages of the flux of the O₂ consuming
 623 processes and of the fractionation factor/coefficients associated with each sequence: $\langle ^{18}\alpha_{\text{total_respi}} \rangle$
 624 and $\langle F_{\text{total_respi}} \rangle$ and $\langle ^{18}\alpha_{\text{total_respi}} \rangle$. We also calculated the net O₂ flux during light periods/period,
 625 $aN = F_{\text{photosynthesis}} - F_{\text{total_respi}}$, as the linear regression, aN , of $\frac{n(O_2)_t}{n(O_2)_{t0}}$ with time. $a^{18}R$ and $a^{18}R$
 626 is also obtained as a linear regression of ^{18}R with time over each light period. Our data support
 627 our assumption that the regime was stationary over time, i.e. that ^{18}R and $n(O_2)_t/n(O_2)_{t0}$
 628 evolved/evolve linearly over time, which is why we were able to do linear regressions.

629

$$^{18}\alpha_{\text{photosynthesis}} = \frac{a^{18}R + aN - \langle ^{18}\alpha_{\text{total_respi}} \rangle \times \langle F_{\text{total_respi}} \rangle}{^{18}R_{lw} \times F_{\text{photosynthesis}}} = \frac{aR^{18} + aN + \langle ^{18}\alpha_{\text{total_respi}} \rangle \times \langle F_{\text{total_respi}} \rangle}{R^{18}O_{lw} \times F_{\text{photosynthesis}}} \quad (2928)$$

631

632

633 We finally estimated a $^{18}\alpha_{\text{photosynthesis}}$ and $^{17}\alpha_{\text{photosynthesis}}$ of 1.0037 and 1.0019, respectively.
 634 Sensitivity tests (Tables S4, S5 and S6) on values of the O₂ flux and associated fractionation coefficients
 635 for photorespiration and Mehler reaction resulted in uncertainty estimates of 0.0012 and 0.0007 for
 636 the values of $^{18}\alpha_{\text{photosynthesis}}$ and $^{17}\alpha_{\text{photosynthesis}}$.

637 The results of the 8 individuals $\alpha_{\text{photosynthesis}}$ values are given in Table S10. (Table S6).

638 ~~The isotopic discriminations $^{18}\epsilon_{\text{photosynthesis}}$ and $^{17}\epsilon_{\text{photosynthesis}}$ were respectively equals to $3.7 \pm$
639 1.3% and $1.9 \pm 0.6 \%$. The average of the gamma value was equal to 0.5207 ± 0.0537 , a value which
640 depends on the value taken for the $\delta^{18}\text{O}$ value of atmospheric air vs VSMOW (Sharp and Wostbrock,
641 2021), see Table 2.~~

642 The value of isotopic fractionation associated with the light period of period 1 of sequence 1 appeared
643 clearly out of range. Following the Dixon's outlier detection test (Dixon, 1960), this value was
644 considered an anomaly (~~with less than 1% likelihood > 99 % of being correct~~) and was removed from
645 further analysis (~~Table S7~~). ~~The individual determination is presented on Table S7.~~

646
647 ~~We finally estimated the values of $^{18}\epsilon_{\text{photosynthesis}}$ and $^{17}\epsilon_{\text{photosynthesis}}$ as $+3.7 \pm 1.3 \%$ and $+1.9$
648 $\pm 0.6 \%$, respectively. The average of $\theta_{\text{photosynthesis}}$ was equal to 0.5207 ± 0.0537 , a value which
649 depends on the value taken for the $\delta^{17}\text{O}$ value of atmospheric O_2 vs VSMOW (Sharp and Wostbrock,
650 2021), see Table 2.~~

651 ~~We performed different sensitivity tests (supplementary texts 1 and 2). Sensitivity test 1 (Table S4)~~
652 ~~quantifies the influence of vanishing flux of dark leaf respiration during the day. This test shows that~~
653 ~~the assumption of similar flux of dark leaf respiration during the night and light periods did not~~
654 ~~influence much the values of photosynthesis fractionation factors. It results in an additional~~
655 ~~uncertainty of 0.0006 and 0.0005 for the values of $^{18}\alpha_{\text{photosynthesis}}$ and $^{17}\alpha_{\text{photosynthesis}}$.~~

656 ~~Sensitivity tests 2 (Tables S7, S8 and S9) were performed on values of the O_2 flux and associated~~
657 ~~fractionation factors for photorespiration and Mehler reaction. They resulted in additional~~
658 ~~uncertainties of 0.0007 and 0.0005 for the values of $^{18}\alpha_{\text{photosynthesis}}$ and $^{17}\alpha_{\text{photosynthesis}}$ (Table~~
659 ~~S10).~~

660 ~~Sensitivity tests 3 concerned the possible evolution of the isotopic composition of leaf water on the~~
661 ~~course of an experiment. The comparison of the $\delta^{18}\text{O}$ of irrigation water and soil water at the end of~~
662 ~~the experiment shows a possible increase up to 2 ‰ (Table S3). We thus estimate that our values of~~
663 ~~leaf water $\delta^{18}\text{O}$ measured at the end of the experiment may be overestimated by 1 ‰ compared to~~
664 ~~the mean value of leaf water $\delta^{18}\text{O}$ during the course of the experiment. Taking this possible effect into~~
665 ~~account would lead to a fractionation factor for photosynthesis higher by 1 ‰ compared to the~~
666 ~~presented one of $3.7 \pm 1.3 \%$, hence a higher isotopic discrimination associated with photosynthesis.~~

667

668 4. Discussion

669 4.1. $\Delta^{17}\text{O}$ of O_2

670 The $\Delta^{17}\text{O}$ of O_2 is equal to 0 by definition for atmospheric air, and hence it should be equal to zero at
 671 the beginning of each experiment. The observed change during an experiment can only be driven by
 672 biological processes ~~because since~~ the interaction with stratosphere is not possible in the closed
 673 chambers.

674 During the soil respiration experimental run, the $\Delta^{17}\text{O}$ of O_2 was constant. This directly reflects the
 675 $\theta_{\text{soil_respi}} \gamma_{\text{soil_respt}}$ value of 0.5164 ± 0.0005 found for respiration (Table 2) ~~because since~~ $\Delta^{17}\text{O}$ of O_2
 676 is defined with a slope of 0.516 between $\ln(1 + \delta^{17}\text{O})$ and $\ln(1 + \delta^{18}\text{O})$ (Eq. 1). This result is in good
 677 agreement and within the uncertainties given by Helman et al. (2005) with the γ value of $0.5174 \pm$
 678 0.0003 obtained with respiration experiments on several micro-organisms.

679 During the experiment involving both oxygen uptake and photosynthesis, the $\Delta^{17}\text{O}$ of O_2 has a globally
 680 increasing trend with values reaching about 100 ppm after one month. Such behavior is expected and
 681 was already observed by Luz et al. (1999) with $\Delta^{17}\text{O}$ of O_2 values reaching 150 ppm after a 200-day
 682 experiment within a closed terrarium. This increase cannot be explained by respiration ~~because since~~
 683 respiration does not modify $\Delta^{17}\text{O}$ of O_2 . It is hence mainly due to photosynthesis producing oxygen
 684 with a $\Delta^{17}\text{O}$ of O_2 different from the atmospheric one. Previous analyses have shown that the $\Delta^{17}\text{O}$ of
 685 H_2O of VSMOW (close to mean oceanic water) expressed vs isotopic composition of atmospheric O_2
 686 has a value between 134 to 223 ppm (using a definition of $\Delta^{17}\text{O}$ of $\text{H}_2\text{O} = \ln(1+\delta^{17}\text{O}) - 0.516 \times \ln(1+\delta^{18}\text{O})$)
 687 (Sharp and Wostbrock, 2021). Within the water cycle, the slopes of $\ln(1+\delta^{17}\text{O})$ vs $\ln(1+\delta^{18}\text{O})$ for the
 688 meteoric line, evaporation and evapotranspiration lines are larger than 0.516 (Li and Meijer, 1998;
 689 Landais et al., 2006) so that $\Delta^{17}\text{O}$ of water consumed by the plants during photosynthesis should be
 690 slightly lower than the $\Delta^{17}\text{O}$ of VSMOW expressed vs isotopic composition of atmospheric O_2 but still
 691 higher than the $\Delta^{17}\text{O}$ of atmospheric O_2 . The photosynthesis is thus responsible for the $\Delta^{17}\text{O}$ of O_2
 692 increase in the closed chamber.

693

694 4.2. Fractionation factors associated with $\delta^{18}\text{O}$ of O_2 and implications for the Dole effect

695 **Table 2. Summary of the mean values of the isotopic discriminations and gamma values for *Festuca***
 696 ***arundinacea* of all sequences of (1) the soil respiration experiment and of (2) the respiration and**
 697 **photosynthesis experiment and the number of data on which they were calculated.**

	Average (‰)	Standard deviation (‰)	Number of data
$\frac{18}{c_{\text{soil_respt}}}$	-12.3	1.7	4
$\frac{17}{c_{\text{soil_respt}}}$	-6.4	0.9	4

γ_{soil_respt}	0.5164	0.0005	4
$^{18}\epsilon_{dark_respt}$	-17.0	2.0	9
$^{17}\epsilon_{dark_respt}$	-8.5	0.8	9
γ_{dark_respt}	0.5124	0.0084	9
$^{18}\alpha_{dark_leave_respt}$	-19.1	2.4	9
$^{17}\alpha_{dark_leave_respt}$	-9.7	0.9	9
$\gamma_{dark_leave_respt}$	0.5089	0.0777	9
$^{18}\epsilon_{photosynthese}$	3.7	1.3	8
$^{17}\epsilon_{photosynthese}$	1.9	0.6	8
$\gamma_{photosynthese}$	0.5207/0.5051**	0.0537/0.0504**	8

698

699

700

701

702

703

** is the value for $\theta_{photosynthesis}\gamma_{photosynthese}$ that depends on the determination of the $\delta^{17}\text{O}$ of atmospheric O_2 vs $\delta^{17}\text{O}$ of VSMOW. We provide here the two different possible estimates using either 12.03 ‰ (Luz and Barkan, 2011) or 12.08 ‰ (Barkan and Luz, 2005): value determined with $\delta^{17}\text{O} = 12.03$ ‰ / value determined with $\delta^{17}\text{O} = 12.08$ ‰.

<u>Isotopic discriminations and gamma values of <i>Festuca arundinacea</i></u>	<u>Average (‰)</u>	<u>Standard deviation (‰)</u>	<u>Number of data</u>
$^{18}\epsilon_{soil_respi}$	-12.3	1.7	4
$^{17}\epsilon_{soil_respi}$	-6.4	0.9	4
θ_{soil_respi}	0.5164	0.0005	4
$^{18}\epsilon_{dark_respi}$	-17.0	2.0	9
$^{17}\epsilon_{dark_respi}$	-8.5	0.8	9
θ_{dark_respi}	0.5124	0.0084	9
$^{18}\alpha_{dark_leaf_respi}$	-19.1	2.4	9
$^{17}\alpha_{dark_leaf_respi}$	-9.7	0.9	9
$\theta_{dark_leaf_respi}$	0.5089	0.0777	9
$^{18}\epsilon_{photosynthesis}$	3.7	1.3	8
$^{17}\epsilon_{photosynthesis}$	1.9	0.6	8
$\theta_{photosynthesis}$	0.5207/0.5051**	0.0537/0.0504**	8

704

705 The isotopic discrimination $^{18}\epsilon_{\text{soil_respi}} = -12.3 \pm 1.7\text{‰}$ for the soil respiration experiments is
706 comparable to the average terrestrial soil respiration isotopic discrimination~~fractionation~~ found by
707 Angert et al. (2001) of -12‰ . Still, among the diversity of soils studied by Angert et al. (2001), the
708 soils showing the $^{18}\epsilon$ values closest to our values are clay soil ($^{18}\epsilon = -13\text{‰}$) and sandy soil ($^{18}\epsilon = -11\text{‰}$).
709 Soil respiration isotopic discriminations are less strong than isotopic discrimination due to dark
710 respiration alone (-18‰, Bender et al., 1994). These lower values for soil respiration isotopic
711 discrimination are due to the roles of root diffusion in the soil (Angert and Luz, 2001). The soils studied
712 by Angert and Luz (2001) are however~~These soils are~~ different from our soil which was enriched in
713 organic matter. Further experiments are then needed to understand the variability in $^{18}\epsilon$ associated
714 with soil respiration.

715 The isotopic discrimination for dark leaf respiration~~in leaf~~, $^{18}\epsilon_{\text{dark_leaf_respi}} - \frac{^{18}\epsilon_{\text{dark_leaf_respi}}}{^{18}\epsilon_{\text{dark_leaf_respi}}} = -$
716 $19.1 \pm 2.4\text{‰}$ is associated with a large uncertainty and would benefit ~~first~~ from additional experiments
717 with a higher sampling and measurement rate. Still, even if it was obtained on different organism and
718 experimental set-up, this value is in agreement with the values for isotopic discrimination for dark
719 respiration determined by Helman et al. (2005) on bacteria from the Lake Kinneret ($^{18}\epsilon = -17.1\text{‰}$) and
720 *Synechocystis* ($^{18}\epsilon = -19.4\text{‰}$ and -19.5‰).

721 The average $^{18}\epsilon_{\text{photosynthesis}}$ is $+3.7 \pm 1.3\text{‰}$ for *Festuca arundinacea* species which goes against the
722 classical assumption that terrestrial photosynthesis does not fractionate (Vinogradov et al., 1959; Guy
723 et al., 1993; Helman et al., 2005; Luz & Barkan, 2005). Vinogradov explains that the low photosynthetic
724 isotopic discrimination that can occur is due to contamination by atmospheric O₂ or by respiration.
725 Guy et al. (1993) corroborate this idea by finding a photosynthetic isotopic discrimination of 0.3‰ in
726 cyanobacteria (*Anacystis nidulans*) and diatoms (*Phaeodactylum tricornutum*) that they consider
727 negligible. Luz and Barkan (2005) in their study on *Philodendron*, consider that there is no
728 photosynthetic isotopic discrimination. Our~~This value~~ proves that there is indeed a terrestrial
729 photosynthetic isotopic discrimination and the value found for *Festuca arundinacea* is slightly~~for the~~
730 isotopic discrimination is smaller than the photosynthetic ~~fractionation~~isotopic discrimination in
731 marine environment $^{18}\epsilon_{\text{photosynthesis}} = +6\text{‰}$ found by Eisenstadt et al. (2010). More specifically,
732 Eisenstadt et al. (2010) determined several photosynthetic isotopic discrimination values depending
733 on the phytoplankton studied (*Phaeodactylum tricornutum* = 4.5‰, *Nannocloreopsis sp.* = 3‰,
734 *Emiliania huxleyi* = 5.5‰ and *Chlamydomonas reinhardtii* = 7‰). One of the conclusions given by
735 Eisenstadt et al. (2010) is that eukaryotic organisms enrich their produced oxygen more in ¹⁸O than
736 prokaryotic organisms. Our conclusion based on experiments performed with *Festuca arundinacea*

737 species is in agreement with these conclusions. We should however note that we tested only one
738 species. Additional experiments with different plants are needed to check if this fractionation factor
739 should be applied for global Dole effect calculation. Still, this positive ¹⁸O discriminations during
740 photosynthesis result suggests that the terrestrial Dole effect may be higher than currently assumed
741 and challenge the assumption that terrestrial and oceanic Dole effects have the same values (Luz and
742 Barkan, 2011).

743

744 4-Conclusion

745 Using a simplified analog of the terrestrial biosphere in a closed chamber we found that the
746 fractionation factors of soil respiration and dark leaf respiration at the biological chamber level agree
747 with the previous estimates derived from studies at micro-organism level ~~studies~~. This is an
748 important confirmatory step for the fractionation factors previously used to estimate the global Dole
749 effect. More importantly, we document for the first time a significant ¹⁸O discrimination~~fractionation~~
750 during terrestrial photosynthesis with the *Festuca arundinacea* species (+ 3.7 ‰ ± 1.3‰). If confirmed
751 by future studies, this can have a substantial impact on the calculation of the Dole effect, with
752 important consequences for our estimates of the past global primary production.

753 Our study showed the usefulness of closed chamber systems to quantify the fractionation factors
754 associated with biological processes in the oxygen cycle at the plant level. The main limitation of our
755 present study was the low sampling rate during our experiments which hamper the precision of the
756 determined fractionation factors. Future work should use this validated set-up to multiply such
757 experiments to improve the precision of fractionation factors and to explore the variability of
758 fractionation factors for different plants and hence different metabolisms. A good application would
759 be to study the difference between C3 and C4 plants because C4 plants do not photorespire. C4 plants,
760 adapted to dry environments, have their own strategy and make very little photorespiration through
761 specialized cells. This allows them to produce their own energy in an optimal way without the waste
762 produced by photorespiration.~~photorespiration.~~

763

764 Data availability

765 All individual fractionation factors for each experiment are given in the Supplement.

766

767 **Author contributions**

768 AL and CPi designed the project. CPi, JS and SD carried out experiments at ECOTRON of Montpellier
769 and FP, CPa, RJ, AD and OJ at LSCE. CPa, NP and AL analyzed the data. CPa and AL prepared the
770 manuscript with contributions from NP, CPi, JS and AM.

771

772 **Competing interests**

773 The authors declare that they have no conflict of interest.

774

775 **Acknowledgements**

776 The research leading to these results has received funding from the European Research Council under
777 the European Union H2020 Programme (H2020/20192024)/ERC grant agreement no. 817493 (ERC
778 ICORDA) and ANR HUM17. The authors acknowledge the scientific and technical support of PANOPLY
779 (Plateforme ANalytique géOsciences Paris-saclaY), Paris-Saclay University, France. This study
780 benefited from the CNRS resources allocated to the French ECOTRONS Research Infrastructure, from
781 the Occitanie Region and FEDER investments as well as from the state allocation ‘Investissement
782 d’Avenir’ AnaEE- France ANR-11-INBS-0001. We would also like to thank Abdelaziz Faez and Olivier
783 Ravel from ECOTRON of Montpellier for their help, ~~and~~ Anne Alexandre from CEREGE at Aix-en-
784 Provence and Emeritus Prof. Phil Ineson from University of York.

785

786 **References**

787 Alexandre, A., Landais, A., Vallet-Coulomb, C., Piel, C., Devidal, S., Pauchet, S., Sonzogni, C., Couapel,
788 M., Pasturel, M., Cornuault, P., Xin, J., Mazur, J-C., Prié, F., Bentaleb, I., Webb, E., Chalié, F., and Roy,
789 J.: The triple oxygen isotope composition of phytoliths as a proxy of continental atmospheric
790 humidity: insights from climate chamber and climate transect calibrations, *Biogeosciences*, 15,
791 3223-3241, <https://doi.org/10.5194/bg-15-3223-2018>, 2018.

792

793 Angert, A., Luz, B., and Yakir, D.: Fractionation of oxygen isotopes by respiration and diffusion in
794 soils and its implications for the isotopic composition of atmospheric O₂, *Global Biogeochem. Cy.*,
795 15, 871-880, <https://doi.org/10.1029/2000GB001371>, 2001.

796

797 Angert, A., Barkan, E., Barnett, B., Brugnoli, E., Davidson, E. A., Fessenden, J., Maneepong, S.,
798 Panapitukkul, N., Randerson, J. T., Savage, K., Yakir, D., and Luz, B.: Contribution of soil respiration in
799 tropical, temperate, and boreal forests to the ^{18}O enrichment of atmospheric O_2 , *Global*
800 *Biogeochem. Cy.*, 17, 1089, <https://doi.org/10.1029/2003GB002056>, 2003.

801

802 Barkan, E., and Luz, B.: High precision measurements of $^{17}\text{O}/^{16}\text{O}$ and $^{18}\text{O}/^{16}\text{O}$ of O_2 and O_2/Ar ratio in
803 air, *Rapid Commun. Mass Spectrom.*, 17, 2809-2814, <https://doi.org/10.1002/rcm.1267>, 2003.

804

805 Barkan, E., and Luz, B.: High precision measurements of $^{17}\text{O}/^{16}\text{O}$ and $^{18}\text{O}/^{16}\text{O}$ ratios in H_2O , *Rapid*
806 *Commun. Mass Spectrom.*, 19, 3737-3742, <https://doi.org/10.1002/rcm.2250>, 2005.

807 [Bauwe, H., Hagemann, M., and Fernie, A.R.: Photorespiration: players, partners and origin, *Trends*](#)
808 [*Plant Sci.*, 6, 330-336, <https://doi.org/10.1016/j.tplants.2010.03.006> , 2010.](#)

809 Bender, M., Sowers, T., Dickson, M-L., Orchardo, J., Grootes, P., Mayewski, P. A., and Meese, D. A.:
810 Climate correlations between Greenland and Antarctica during the past 100,000 years, *Nature*, 372,
811 663-666, <https://doi.org/10.1038/372663a0>, 1994.

812

813 Blunier, T., Barnett, B., Bender, M. L., and Hendricks, M. B.: Biological oxygen productivity during the
814 last 60,000 years from triple oxygen isotope measurements, *Global Biogeochem. Cy.*, 16, 3-4,
815 <https://doi.org/10.1029/2001GB001460>, 2002.

816

817 Brandon, M., Landais, A., Duchamp-Alphonse, S., Favre, V., Schmitz, L., Abrial, H., Prié, F., Extier, T.,
818 and Blunier, T.: Exceptionally high biosphere productivity at the beginning of Marine Isotopic Stage
819 11, *Nat. Commun.*, 11, 1-10, <https://doi.org/10.1038/s41467-020-15739-2>, 2020.

820

821 [Dansgaard, W.: Stable isotopes in precipitation, *Tellus*, 16, 436-468, 1974.](#)

822

823 [Davidson, E.A., Janssens, I.A., and Luo, Y.: On the variability of respiration in terrestrial](#)
824 [ecosystems:moving beyond Q10, *Glob. Change Biol.*, 12, 154-164,](#)
825 [<https://doi.org/10.1111/j.1365-2486.2005.01065.x>, 2005.](#)

826

827 Dixon, W. J.: Simplified estimation from censored normal sample, *Ann. Math. Stat.*, 21, 488-506,
828 <https://doi.org/10.1214/aoms/1177729747>, 1960.

829

830 Dole, M., Lane, G. A., Rudd, D. P., and Zaukelies, D. A.: Isotopic composition of atmospheric oxygen
831 and nitrogen, *Geochim. Cosmochim. Ac.*, 6, 65-78, [https://doi.org/10.1016/0016-7037\(54\)90016-2](https://doi.org/10.1016/0016-7037(54)90016-2),
832 1954.

833

834 [Dongman, G., Nürnberg, H. W., Förstel, H., and Wagener, K.: On the enrichment of H₂¹⁸O in the](#)
835 [leaves of transpiring plants, *Radiat Environ Biophys*, 11, 41-52,](#)
836 <https://doi.org/10.1007/BF01323099>, 1974.

837

838 Dreyfus, G. B., Parrenin, F., Lemieux-Dudon, B., Durand, G., Masson-Delmotte, V., Jouzel, J.,
839 Barnola³, J.-M., Panno⁵, L., Spahni, R., Tisserand, A., Siegenthaler, U., and Leuenberger, M.:
840 Anomalous flow below 2700 m in the EPICA Dome C ice core detected using $\delta^{18}\text{O}$ of atmospheric
841 oxygen measurements, *Clim. Past*, 3, 341-353, <https://doi.org/10.5194/cp-3-341-2007>, 2007.

842

843 Eisenstadt, D., Barkan, E., Luz, B., and Kaplan, A.: Enrichment of oxygen heavy isotopes during
844 photosynthesis in phytoplankton, *Photosynth. Res.*, 103, 97-103,
845 <https://doi.org/10.1007/s11120-009-9518-z>, 2010.

846

847 Extier, T., Landais, A., Bréant, C., Prié, F., Bazin, L., Dreyfus, G., Roche, D. M., Leuenberger, M.: On
848 the use of $\delta^{18}\text{O}_{\text{atm}}$ for ice core dating, *Quat. Sci. Rev.*, 185, 244-257,
849 <https://doi.org/10.1016/j.quascirev.2018.02.008>, 2018.

850

851 Guy, R. D., Fogel, M.L., and Berry, J. A.: Photosynthetic fractionation of the stable isotopes of oxygen
852 and carbon, *Plant Physiol.*, 101, 37-47, <https://doi.org/10.1104/pp.101.1.37>, 1993.

853

854 Helman, Y., Barkan, E., Eisenstadt, D., Luz, B., and Kaplan, A.: Fractionation of the three stables
855 oxygen isotopes by oxygen-producing and oxygen-consuming reactions in photosynthetic
856 organisms, *Plant Physiol.*, 138, 2292-2298, <https://doi.org/10.1104/pp.105.063768>, 2005.

857

858 Hillaire-Marcel, C., Kim, S.-T., Landais, A., Ghosh, P., Assonov, S., Lécuyer, C., Blanchard, M., Meijer,
859 H. A. J., and Steen-Larsen, H.: A stable isotope toolbox for water and inorganic carbon cycle studies,
860 *Nat. Rev. Earth Environ*, 2, 699-719, <https://doi.org/10.1038/s43017-021-00209-0>, 2021.

861

862 Hoffmann, G., Cuntz, M., Weber, C., Ciais, P., Friedlingstein, P., Heimann, M., Jouzel, J., Kaduk, J.,
863 Maier Reimer, E., Seibt, U., and Six, K.: A model of the Earth's Dole effect, *Global Biogeochem. Cy.*,
864 18, 1-15, <https://doi.org/10.1029/2003GB002059>, 2004.

865 [Keenan, T.F., Migliavacca M., Papale, D., Baldocchi, D., Reichstein, M., Torn, M., and Wutzler, T.:](#)
866 [Widespread inhibition of daytime ecosystem respiration, *Nat. Ecol. Evol.*, 3, 407-415,](#)
867 <https://doi.org/10.1038/s41559-019-0809-2>, 20194.

868
869 Landais, A., Barkan, E., Yakir, D., and Luz, B.: The triple isotopic composition of oxygen in leaf water,
870 *Geochim. Cosmochim. Ac.*, 70, 4105-4115, <https://doi.org/10.1016/j.gca.2006.06.1545>, 2006.

871
872 Landais, A., Dreyfus, G., Capron, E., Masson-Delmotte, V., Sanchez-Goñi, M. F., Desprat, S.,
873 Hoffmann, G., Jouzel, J., Leuenberger and M., Johnsen, S.: What drives the orbital and millennial
874 variations of $d^{18}O_{atm}$?, *Quat. Sci. Rev.*, 29, 235-246, <https://doi.org/10.1016/j.quascirev.2009.07.005>,
875 2010.

876
877 Luz, B., and Barkan, E.: The isotopic composition of atmospheric oxygen, *Global Biogeochem. Cy.*,
878 25, GB3001, <https://doi.org/10.1029/2010GB003883>, 2011.

879
880 Luz, B., Barkan, E., Bender, M. L., Thiemens, M. H., and Boering, K. A.: Triple-isotope composition of
881 atmospheric oxygen as a tracer of biosphere productivity, *Nature*, 400, 547-550,
882 <https://doi.org/10.1038/22987>, 1999.

883
884 Malaizé, B., Paillard, D., Jouzel, J., and Raynaud, D.: The Dole effect over the Last two glacial-
885 interglacial cycles, *J. Geophys. Res.*, 104, 14199-14208, <https://doi.org/10.1029/1999JD900116>,
886 1999.

887 Mehler, A.: Studies on reactions of illuminated chloroplasts: I. Mechanism of the reduction of
888 oxygen and other hill reagents, *Arch. Biochem. Biophys.*, 33, 65-77,
889 [https://doi.org/10.1016/00039861\(51\)90082-3](https://doi.org/10.1016/00039861(51)90082-3), 1951.

890
891 Meijer, H. A. J., and Li, W. J.: The use of electrolysis for accurate $\delta^{17}O$ and $\delta^{18}O$ Isotope
892 Measurements in Water, *Isot. Environ. Health Stud.*, 34, 349-369,
893 <https://doi.org/10.1080/10256019808234072>, 1998.

894
895 Milcu, A., Allan, E., Roscher, C., Jenkins, T., Meyer, S. T., Flynn, D., Bessler, H., Buscot, F.,
896 Engels, C., Gubsch, M., König, S., Lipowsky, A., Loranger, J., Renker, C., Scherber, C., Schmid,
897 B., Thébault, E., Wubet, T., Weisser, W. W., Scheu, S., and Eisenhauer, N.: Functionally and
898 phylogenetically diverse plant communities key to soil biota, *Ecology*, 94, 1878-1885,

899 [https://doi.org/ 10.1890/12-1936.1](https://doi.org/10.1890/12-1936.1), 2013.

900

901 Reutenauer, C., A. Landais, A., T. Blunier, T., C. Bréant, C., M. Kageyama, M., M.-N. Woillez, M.-N.,
902 Risi, C., Mariotti, V., and P. Braconnot, Quantifying molecular oxygen isotope variations during a
903 Heinrich stadial, *Clim. Past*, 11, 1527-1551, <https://doi.org/10.5194/cp-11-1527-2015>, 2015.

904

905 Ribas-Carbo, M., Berry, J.A., Yakir, D., Giles, L., Robinson, S.A., Lennon, A.M., and Siedow, J.N.:
906 Electron Partitioning between the Cytochrome and Alternative Pathways in Plant
907 Mitochondria, *Plant Physiol.*, 109, 829-837, <https://doi.org/10.1104/pp.109.3.829>, 1995.

908

909 Seltzer, A. M., Severinghaus, J. P., Andraski, B. J., and Stonestrom, D. A.: Steady state
910 fractionation of heavy noble gas isotopes in a deep unsaturated zone, *Water Resour. Res.*, 53,
911 2716-2732, <https://doi.org/10.1002/2016WR019655>, 2017.

912

913 Severinghaus, J. P., Beaudette, R., Headly, M. A., Taylor, K. and Brook, E. J.: Oxygen-18 of O₂ records
914 the impact of abrupt climate change on the terrestrial biosphere, *Science*, 324, 1431-1434,
915 <https://doi.org/10.1126/science.1169473>, 2009.

916

917 Shackleton, N. J.: The 100,000-Year Ice-Age Cycle Identified and Found to Lag Temperature,
918 Carbon Dioxide, and Orbital Eccentricity, *Science*, 289, 1897-1902,
919 <https://doi.org/10.1126/science.289.5486.1897>, 2000.

920

921 Sharkey, T.D., Badger, M.R., von Caemmerer, S., and Andrews, T.J.: High Temperature Inhibition of
922 Photosynthesis Requires Rubisco Activase for Reversibility, *Trends Plant Sci.*, 2465-2468,
923 https://doi.org/10.1007/978-94-011-3953-3_577, 1998.

924

925 Sharp, Z. D., and Wostbrock, J. A. G.: Standardization for the Triple Oxygen Isotope System: Waters,
926 Silicates, Carbonates, Air, and Sulfates, *Rev. Mineral. Geochem.*, 86, 179-196,
927 <https://doi.org/10.2138/rmg.2021.86.05>, 2021.

928

929 Stolper, D. A., Fischer, W. W., and Bender, M. L.: Effects of temperature and carbon source on the
930 isotopic fractionations associated with O₂ respiration for ¹⁷O/¹⁶O and ¹⁸O/¹⁶O ratios in *E.*
931 *coli*, *Geochim. Cosmochim. Ac.*, 240, 152-172, <https://doi.org/10.1016/j.gca.2018.07.039>, 2018.

932 [Tcherkez, G., and Farquhar, G.D.: On the ¹⁶O/¹⁸O isotope effect associated with photosynthetic O₂](#)
933 [production, *Funct. Plant Biol.*, 34, 1049-1052, <https://doi.org/10.1071/FP07168>, 2007.](#)

934 [Tcherkez, G., Gauthier, P., Buckley, T.N, Bush, F.A., Barbour, M.M., Bruhn, D., Heskell, M.A., Gong, X.Y.,](#)
935 [Crous, K.Y., Griifin, K., Way, D., Turnbull, M., Adams, M.A., Atkin, O.K., Farquhar, G.D., and Cornic, G.:](#)
936 [Leaf day respiration: low CO₂ flux but high significance for metabolism and carbon balance, *New*](#)
937 [*Phytol.*, 216, 986-1001, <https://doi.org/10.1111/nph.14816>, 2017.](#)

938 [Vinogradov, A. P., Kutyurin, V.M., and Zadorozhnyi, I.K.: Isotope fractionation of atmospheric oxygen,](#)
939 [*Geochem. Int.*, 3, 241-253, 1959.](#)

940 Wang, Y., Cheng, H., Lawrence Edwards, R., Kong, X., Shao, X., Chen, S., Wu, J., Jiang, X., Wang, X.,
941 and An, Z.: Millennial- and orbital-scale changes in the East Asian monsoon over the past 224,000
942 years, *Nature*, 451, 1090-1093, <https://doi.org/10.1038/nature06692>, 2008.

943

944